PLOS COMPUTATIONAL BIOLOGY

RESEARCH ARTICLE

Selection for rapid uptake of scarce or fluctuating resource explains vulnerability of glycolysis to imbalance

Albertas Janulevicius*, G. Sander van Doorn

Groningen Institute for Evolutionary Life Sciences, University of Groningen, the Netherlands

* albertas.janulevicius@gmail.com

OPEN ACCESS

Citation: Janulevicius A, van Doorn GS (2021) Selection for rapid uptake of scarce or fluctuating resource explains vulnerability of glycolysis to imbalance. PLoS Comput Biol 17(1): e1008547. https://doi.org/10.1371/journal.pcbi.1008547

Editor: Pedro Mendes, University of Connecticut School of Medicine, UNITED STATES

Received: February 6, 2020

Accepted: November 16, 2020

Published: January 19, 2021

Data Availability Statement: All relevant data are within the manuscript and its Supporting information files.

Funding: This work was financially supported by the Netherlands Organisation for Scientific Research (NWO Vidi Grant 864.11.012 to GSvD) and the European Research Council (ERC Starting Grant 309555 to GSvD). The funders had no role in study design, data collection and analysis, decision to publish, or preparation of the manuscript.

Competing interests: The authors have declared that no competing interests exist.

Abstract

Glycolysis is a conserved central pathway in energy metabolism that converts glucose to pyruvate with net production of two ATP molecules. Because ATP is produced only in the lower part of glycolysis (LG), preceded by an initial investment of ATP in the upper glycolysis (UG), achieving robust start-up of the pathway upon activation presents a challenge: a sudden increase in glucose concentration can throw a cell into a self-sustaining imbalanced state in which UG outpaces LG, glycolytic intermediates accumulate and the cell is unable to maintain high ATP concentration needed to support cellular functions. Such metabolic imbalance can result in "substrate-accelerated death", a phenomenon observed in prokaryotes and eukaryotes when cells are exposed to an excess of substrate that previously limited growth. Here, we address why evolution has apparently not eliminated such a costly vulnerability and propose that it is a manifestation of an evolutionary trade-off, whereby the glycolysis pathway is adapted to quickly secure scarce or fluctuating resource at the expense of vulnerability in an environment with ample resource. To corroborate this idea, we perform individual-based eco-evolutionary simulations of a simplified yeast glycolysis pathway consisting of UG, LG, phosphate transport between a vacuole and a cytosol, and a general ATP demand reaction. The pathway is evolved in constant or fluctuating resource environments by allowing mutations that affect the (maximum) reaction rate constants, reflecting changing expression levels of different glycolytic enzymes. We demonstrate that under limited constant resource, populations evolve to a genotype that exhibits balanced dynamics in the environment it evolved in, but strongly imbalanced dynamics under ample resource conditions. Furthermore, when resource availability is fluctuating, imbalanced dynamics confers a fitness advantage over balanced dynamics: when glucose is abundant, imbalanced pathways can quickly accumulate the glycolytic intermediate FBP as intracellular storage that is used during periods of starvation to maintain high ATP concentration needed for growth. Our model further predicts that in fluctuating environments, competition for glucose can result in stable coexistence of balanced and imbalanced cells, as well as repeated cycles of population crashes and recoveries that depend on such polymorphism. Overall, we demonstrate the importance of ecological and evolutionary arguments for understanding seemingly maladaptive aspects of cellular metabolism.

Author summary

Glycolysis is a central pathway in cellular energy metabolism that breaks down glucose to produce ATP, yet it can sometimes fail to start up properly after cells have experienced a period of starvation. This puzzling failure occurs when a sudden increase in glucose concentration throws a cell into a self-sustaining imbalanced state in which upper and lower glycolysis work at different rates. As a result, glycolytic intermediates accumulate in the cell, and it is unable to maintain high ATP concentration needed to support cellular functions. Here, we perform individual-based eco-evolutionary simulations of a simplified yeast glycolysis pathway and show that this apparently costly vulnerability allows for faster growth in environments with scarce or fluctuating resource availability. Accordingly, we propose that vulnerability to metabolic imbalance can be interpreted as a manifestation of an evolutionary trade-off between performance in rich, stable environments and poor, fluctuating ones. Furthermore, we show that when resource availability fluctuates, imbalanced dynamics itself can be advantageous: when glucose is abundant, imbalanced pathways can quickly accumulate glycolytic intermediates as intracellular storage that is used to sustain growth during periods of starvation. Finally, we find that in variable environments, competition for glucose can support stable coexistence of balanced and imbalanced cells in the population, as well as repeated cycles of population crashes and recoveries. Overall, our results show that ecological and evolutionary mechanisms provide a fruitful context for interpreting seemingly flawed aspects of cellular metabolism.

Introduction

In many organisms, glycolysis is an essential pathway in energy metabolism that converts glucose to pyruvate with net production of two ATP molecules per glucose molecule [1]. Net formation of ATP occurs in the lower part of glycolysis (LG) which is preceded by an initial investment of ATP in the upper part of glycolysis (UG). Such a "turbo design" of the pathway carries an inherent risk: a sudden increase in glucose levels can push the pathway into a self-sustaining imbalanced state, where UG outpaces LG, glycolytic intermediates accumulate and the cell is unable to maintain high ATP concentration needed to support cellular functions [2, 3]. In yeast, such a phenotype is usually associated with mutants of the trehalose metabolism [2, 4, 5]. However, wild-type (WT) yeast cells are vulnerable as well: a switch of growth substrate from galactose to glucose renders 7 % of cells non-viable [3]. A yeast cell trapped in the imbalanced state will restore metabolic balance and resume growth if glucose is removed within several hours, but the cell will die if the imbalance continues [3]. This is an example of substrate-accelerated death, a wider phenomenon observed in prokaryotes and eukaryotes when cells are unable to grow when exposed to excess substrate that previously limited growth [6–8].

The co-occurrence of a balanced and an imbalanced state in yeast glycolysis is well captured by a generalized core glycolysis model (Fig 1A) developed previously by van Heerden et al. [3] The model predicts two stable states, one yielding a steady-state concentration of the intermediate metabolite fructose-1,6-bisphosphate (FBP) and a high ATP concentration (balanced state), and the other characterized by steady accumulation of FBP and depletion of ATP and intracellular inorganic phosphate pools (imbalanced state). The key factor determining the fate of the system is the dynamics of inorganic phosphate (P_i) during the start-up of glycolysis. According to the model, the transition to excess glucose proceeds as follows [3]. Upon sudden

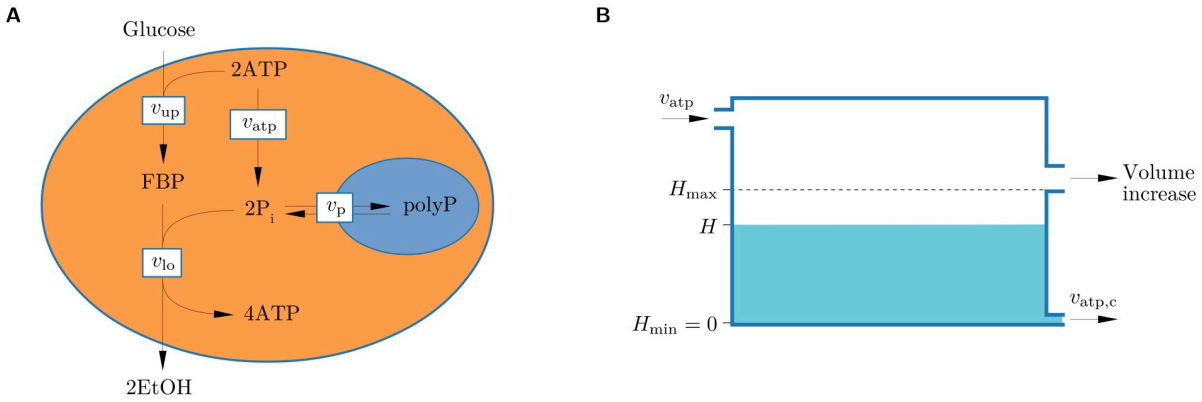

Fig 1. A model of a yeast cell with a simplified glycolysis pathway. (A) A generalized core model of yeast glycolysis [3] considers the intracellular concentrations of the glycolytic intermediate fructose-1,6-bisphosphate (FBP), ATP and inorganic phosphate (P_i), and four reactions (arrows): (i) a lumped upper glycolysis reaction that produces FBP from extracellular glucose with rate v_{up}, (ii) a lumped lower glycolysis reaction that generates ATP and the waste product ethanol (EtOH) at rate v_{lo}, (iii) ATPase reaction reflecting general ATP demand in the cell at rate v_{atp}, and (iv) reversible phosphate transport between the cytosol and the vacuole at rate v_p. PolyP refers to the vacuolar store of polyphosphate. (B) The flux through the ATPase reaction v_{atp} and the associated cell growth rate can be visualized by water flow through a tank with two outlets. v_{atp} is coupled to cell growth in a way that allows a cell to survive and recover from limited periods of negative energy balance (e.g., during metabolic imbalance or starvation). The coupling is mediated via cellular reserves, quantified by a variable H (cell health, depicted by the water level in the tank). A cell grows (increases in volume) when its health H is at the maximal value and v_{atp} is larger than obligatory cellular maintenance cost $v_{atp,c}$. When v_{atp} is not sufficient to cover cellular maintenance cost, cell health decreases. The cell dies if its health drops to zero.

https://doi.org/10.1371/journal.pcbi.1008547.g001

glucose exposure, the rate of UG initially exceeds that of LG ($v_{up} > v_{lo}$), causing FBP to increase. For a balanced steady state, v_{lo} has to accelerate and catch up with v_{up}. This challenge is more difficult if UG activity (v_{up}) is higher, e.g. due to a higher expression level of UG enzymes or higher glucose concentration. Accumulation of FBP binds P_i and will cause a drop in its concentration in the cytosol. Because both FBP and P_i are substrates for LG, the increase in FBP will tend to speed up v_{lo}, whereas the associated decrease in P_i will tend to slow it down. Which of these two effects is dominant determines the trajectory of the system. If P_i concentration remains sufficiently high, v_{lo} will increase to become equal with v_{up}, and a balanced steady state will be established. Otherwise, P_i will become a limiting factor for LG and v_{lo} will not accelerate fast enough to catch up with v_{up}, causing the system to collapse into the imbalanced state. Once caught in the imbalanced state, cells are trapped, because P_i mobilized from the vacuole maintains the imbalance: at low concentrations of P_i and ATP, an imported P_i molecule enhances v_{lo}, but the concomitant production of 2 ATP molecules increases v_{up} twice as much as v_{lo}. Given that imbalanced cells exist in an alternative stable metabolic state, random initial variation in enzyme and metabolite concentrations can be enough to drive a subpopulation of cells into the imbalanced state. This explains why both balanced and imbalanced cells can be present in an isogenic population upon transition to excess glucose after starvation [3].

van Heerden et al. suggest that vulnerability of glycolysis to imbalance arises from the fundamental design of the pathway and cannot be fully prevented by regulatory mechanisms [3]. However, their analysis of the full kinetic glycolysis model shows that quicker liberation of P_i by enhancing ATPase activity, activation of the glycerol formation branch, futile trehalose cycling, or quicker import of P_i into the cytosol from the vacuole can all markedly decrease the probability of reaching the imbalanced state [3]. Furthermore, the presence of trehalose cycling combined with experimentally observed trehalose-6-phosphate mediated inhibition of hexokinase [9] can remove the existence of metabolic imbalance in the model altogether. It is

therefore puzzling that 7 % of WT yeast cells fall into the imbalanced state upon a sudden increase in glucose availability. Why have WT cells not evolved such mechanisms to completely eliminate the risk of imbalance? One possible evolutionary explanation is that although imbalanced v_{up} and v_{lo} are dangerous to the cell, regulatory mechanisms to keep them tightly balanced, or constitutive higher expression of LG enzymes are just too costly relative to the fitness benefit of avoiding substrate-accelerated death. Yet, given the potential of a 7 % increase in survival, these costs must be assumed to be substantial. An alternative hypothesis that we propose here is that imbalanced v_{up} and v_{lo} are not always detrimental to the cell, but may, in fact, be adaptive under a range of natural conditions. In particular, allocating a larger fraction of enzymatic capacity to UG at the expense of LG would allow cells to acquire glucose from the environment faster, increasing their competitive advantage under conditions of low resource availability. Moreover, in variable environments, glucose may normally run out before metabolic imbalance becomes irreversible, so that periods of starvation would restore normal levels of glycolytic intermediates and cells would be protected from substrate-accelerated death. From this perspective, the vulnerability of cells to fall into the imbalanced state in rich and constant environments (e.g., typical lab conditions) can be interpreted as the result of an evolutionary trade-off: adaptations of the glycolysis pathway that improve its performance under conditions of low or varying glucose make it vulnerable to imbalance at constant high glucose concentrations. In other words, we suggest that imbalanced dynamics in WT yeast cells are observed because cells are adapted to a different glucose availability regime than the one used in the experiments [3].

To investigate this idea, we performed evolutionary simulations of a population of yeast cells with the simplified yeast glycolysis pathway shown in Fig 1A, subject to different glucose availability regimes. Variation in the population was introduced by mutating (maximum) reaction rate constants of the pathway, reflecting changing expression levels of the glycolytic enzymes. Cells contributed to future generations in proportion to their growth rate, so that natural selection acted on the simulated populations to improve the functionality of the pathway in the current environment. We then quantified the likelihood of cells with the evolved pathways to fall into the imbalanced state upon transitioning to excess glucose. Our results demonstrate that the regime of glucose availability that cells have previously adapted to has a marked effect on their measure of balancedness. The model also predicts a range of environmental conditions where balanced and imbalanced cells can stably coexist in the population, and where such polymorphism drives periodic crashes and recoveries of the population. We discuss these results in relation to the tragedy of the commons and evolutionary suicide to illustrate how eco-evolutionary mechanisms can shed new light on seemingly maladaptive aspects of cellular metabolism.

Model and methods

Model description

We model a population of yeast cells that metabolize glucose in a chemostat under anaerobic conditions. To model glycolysis, we employ a generalized core model [3] comprising four reactions (Fig 1A and S1 Model), with the addition of explicit glucose dynamics and phosphate depletion from the yeast vacuole:

i. Upper glycolysis is modeled to exhibit irreversible two-substrate Michaelis-Menten kinetics. Phosphofructokinase, an enzyme of upper glycolysis, is allosterically inhibited by ATP [1, 10, 11], hence the reaction rate of upper glycolysis v_{up} contains an inhibition term with the

inhibitor constant $K_{i,atp}$ for ATP:

$$v_{up} = \frac{v_{max,up}[Glc][ATP]}{\left(K_{M,glc} + [Glc]\right)\left(K_{M,atp} + [ATP]\left(1 + \frac{[ATP]}{K_{i,atp}}\right)\right)}, \quad (1)$$

where $v_{max,up}$ is maximal upper glycolysis rate, $K_{M,glc}$ and $K_{M,atp}$ are the Michaelis constants for glucose and ATP, respectively (similar notations are used below for corresponding parameters in other reactions).

ii. Lower glycolysis is assumed to follow irreversible three-substrate Michaelis-Menten kinetics. Its rate, v_{lo}, is given by

$$v_{lo} = \frac{v_{max,lo}[FBP][ADP][P_i]}{(K_{M,fbp} + [FBP])(K_{M,adp} + [ADP])(K_{M,p} + [P_i])}, \quad (2)$$

where [ADP] is found from a conserved quantity a_{tot} = [ATP]+ [ADP].

iii. ATP consumption by all kinds of cellular processes (ATP demand) is modeled by a general ATPase reaction that follows first-order reaction kinetics with rate

$$v_{atp} = k_{atp}[ATP] \quad (3)$$

and reaction rate constant k_{atp}.

iv. Phosphate is transported between the vacuole and the cytosol at rate

$$v_p = k_p([P_i]_{vac} - [P_i]), \quad (4)$$

where $[P_i]$ and $[P_i]_{vac}$ are the phosphate concentration in the cytosol and the vacuole, respectively, and k_p is the reaction rate constant. When $[P_i] < [P_i]_{vac}$, phosphate is transported from the vacuole into the cytosol ($v_p > 0$), and in the opposite direction when $[P_i] > [P_i]_{vac}$ ($v_p < 0$). It has been observed that glycolytic intermediates accumulate in cells that undergo imbalanced dynamics until all phosphate from the vacuole is depleted [3, 4, 9]. Furthermore, phosphate in the vacuole is stored as polyphosphate; we therefore assume that the vacuolar phosphate concentration $[P_i]_{vac}$ is buffered [3, 12]. Thus the depletion of phosphate from the vacuole is modeled by assuming that $[P_i]_{vac}$ drops as the total concentration of phosphate imported into the cytosol $[P_{tot}] = [P_i] + 2[FBP] + [ATP]$ increases:

$$[P_i]_{vac} = \frac{[P_i]_{vac,max}}{1 + \left(\frac{[P_{tot}]}{K_{vac}}\right)^m}, \quad (5)$$

where $[P_i]_{vac,max}$ is the phosphate concentration in the vacuole when no phosphate in the cytosol is present, K_{vac} is the total concentration of phosphate in the cytosol that reduces $[P_i]_{vac}$ to one half of $[P_i]_{vac,max}$, and $m > 0$ determines whether phosphate depletion sets in gradually (small m) or suddenly (large m). In this way, K_{vac} models the size of the vacuolar phosphate store, or, more generally, the capacity of the cell to accumulate FBP during glycolytic imbalance.

Metabolite concentrations in the cell are affected not only by glycolysis reactions, but also by dilution due to the increase in volume V of a growing cell. While this effect is often ignored in metabolic models, we included it here, because we track cells over entire generations, involving a substantial change of cell volume and accumulation of metabolites. The decrease

in metabolite concentration c due to dilution can be found from the conservation of the amount of metabolite cV in the cell as its volume increases:

$$(cV)' = c'V + cV' = 0 \Rightarrow c' = -c\frac{V'}{V}\,, \tag{6}$$

where the derivatives (denoted by the prime symbol) are with respect to time.

The dynamics of metabolites that participate in glycolysis reactions in a growing cell are thus governed by the following ordinary differential equations:

$$\begin{aligned}
[\mathrm{FBP}]' &= \nu_{\mathrm{up}} - \nu_{\mathrm{lo}} - [\mathrm{FBP}]\frac{V'}{V}\,,\\
[\mathrm{ATP}]' &= -2\nu_{\mathrm{up}} + 4\nu_{\mathrm{lo}} - \nu_{\mathrm{atp}} - [\mathrm{ATP}]\frac{V'}{V}\,,\\
[\mathrm{P_i}]' &= -2\nu_{\mathrm{lo}} + \nu_{\mathrm{atp}} + \nu_{\mathrm{p}} - [\mathrm{P_i}]\frac{V'}{V}\,.
\end{aligned} \tag{7}$$

(Since a_{tot} = [ATP]+ [ADP] is constant, these equations implicitly incorporate the production of ADP in growing cells by other components of cellular metabolism to compensate for its dilution).

Four of the parameters of the metabolic pathway, $\nu_{\mathrm{max,up}}$, $\nu_{\mathrm{max,lo}}$, k_{atp} and k_{p}, reflect the expression levels of respective enzymes (i.e., their concentrations) and are taken to be evolvable parameters that define the genotype of the model cell. Since we aim to study evolutionary adaptation of the metabolic pathway, we must next specify its connection to growth and survival, the two key components of cellular fitness. These fitness characteristics, together with the nature of metabolite dynamics (balanced, imbalanced or intermediate) constitute the phenotype of the cell. In our model, glycolysis is coupled to growth and survival by the general ATPase reaction. It is assumed that all generated ATP is used up by a cell. This assumption is valid not only under energy (glucose) limitation conditions, but also under energy surplus, because our model includes an element of control of the glycolytic flux by demand, i.e., UG is inhibited by high ATP concentrations (Eq 1) [13]. As a result, the growth rate of a cell with balanced metabolism is coupled to its rate of glucose uptake. We also assume that the flux through the ATPase reaction (ν_{atp}) is first allocated to cover cellular maintenance costs ($\nu_{\mathrm{atp,c}}$) and that any remaining flux ($\nu_{\mathrm{atp,g}}$) is invested in cell growth, i.e. the production of new cell biomass, which leads to an increase in cell volume V(Fig 1B and S1 Model). The maintenance costs are further decomposed into $\nu_{\mathrm{atp,e}}$, the ATP demand required for expressing the glycolytic enzymes, which therefore may vary between cell genotypes, and the ATP required by other transcription and general cell maintenance processes ($\nu_{\mathrm{atp,m}}$), which is assumed to be equal between genotypes. Hence,

$$\nu_{\mathrm{atp}} = \nu_{\mathrm{atp,c}} + \nu_{\mathrm{atp,g}} = (\nu_{\mathrm{atp,e}} + \nu_{\mathrm{atp,m}}) + \nu_{\mathrm{atp,g}}\,. \tag{8}$$

Because the cell maintenance flux $\nu_{\mathrm{atp,c}}$ is an obligatory component of the energy budget, cells are faced with an energy deficit when $\nu_{\mathrm{atp}} < \nu_{\mathrm{atp,c}}$ (or, equivalently, when $\nu_{\mathrm{atp,g}} < 0$). This occurs at low intracellular ATP concentration during periods of starvation or glycolytic imbalance. We assume that cells can buffer short periods of negative energy balance by drawing on internal reserves, but that they eventually die when starvation or imbalance persists. To model the deteriorating condition of a starving cell, we introduce a variable H that reflects cell health. Cell health decreases when ATP production falls short of meeting the energy demands for maintenance (i.e., when $\nu_{\mathrm{atp,g}} < 0$). A cell dies when H decreases to $H_{\mathrm{min}} = 0$, but, if starvation ends before this point is reached, the cell can recover. In fact, when $\nu_{\mathrm{atp,g}}$ becomes positive

after a period of starvation, it is first invested into replenishing the internal reserves (modeled as an increase in H). When a cell is at its maximum health $H_{\max}$, and $v_{\mathrm{atp,g}} > 0$, the cell will increase in volume (Fig 1B). We assume that the amount of ATP needed to produce a unit of new cell volume is constant and independent of cell volume or genotype. In other words, the increase in cell volume is proportional to the total amount of ATP converted by the flux $v_{\mathrm{atp,g}}$ in the cell,

$$V' \propto v_{\mathrm{atp,g}} V \Rightarrow \frac{V'}{V} \propto v_{\mathrm{atp,g}}\,, \tag{9}$$

i.e. the rate of increase in the fractional cell volume is proportional to $v_{\mathrm{atp,g}}$. This will yield an exponential increase in cell volume at constant $v_{\mathrm{atp,g}}$, consistent with experimental measurements of yeast cell growth [14].

To find the proportionality constant, we assume that a cell with the reference genotype reported by Heerden et al. [3] ($v^{\mathrm{r}}_{\mathrm{max,up}}$, $v^{\mathrm{r}}_{\mathrm{max,lo}}$, $k^{\mathrm{r}}_{\mathrm{atp}}$ and $k^{\mathrm{r}}_{\mathrm{p}}$) undergoing balanced glycolysis in an environment with constant 2 mM glucose will double its volume in time τ_{g}. Since under these conditions the ATP demand is $v^{\mathrm{r,b}}_{\mathrm{atp}}$, the expression cost of the reference genotype $v^{\mathrm{r}}_{\mathrm{atp,e}}$ is chosen to yield a positive reference growth flux $v^{\mathrm{r,b}}_{\mathrm{atp,g}} = v^{\mathrm{r,b}}_{\mathrm{atp}} - (v^{\mathrm{r}}_{\mathrm{atp,e}} + v_{\mathrm{atp,m}})$ (Table 1). The dynamics of cell growth in our model is therefore

$$\frac{V'}{V} = \begin{cases} u_{\mathrm{g}} \cdot v_{\mathrm{atp,g}} & \text{if } H = H_{\max} \text{ and } v_{\mathrm{atp,g}} > 0\,, \\ 0 & \text{otherwise}\,, \end{cases} \tag{10}$$

where

$$u_{\mathrm{g}} = \frac{\ln 2}{\tau_{\mathrm{g}} \cdot v^{\mathrm{r,b}}_{\mathrm{atp,g}}}\,.$$

Cell health dynamics is similarly scaled by assuming that a cell with the reference genotype in an imbalanced state will die in time τ_{d}. Under these conditions, a cell with a reference genotype has a small ATPase flux $v^{\mathrm{r,i}}_{\mathrm{atp}}$ and thus a negative reference growth flux $v^{\mathrm{r,i}}_{\mathrm{atp,g}} = v^{\mathrm{r,i}}_{\mathrm{atp}} - (v^{\mathrm{r}}_{\mathrm{atp,e}} + v_{\mathrm{atp,m}})$. Cell health dynamics is therefore

$$H' = \begin{cases} -u_{\mathrm{d}} \cdot v_{\mathrm{atp,g}} & \text{if } v_{\mathrm{atp,g}} \leq 0\,, \\ u_{\mathrm{g}} \cdot v_{\mathrm{atp,g}} & \text{if } v_{\mathrm{atp,g}} > 0 \text{ and } H < H_{\max}\,, \\ 0 & \text{if } v_{\mathrm{atp,g}} > 0 \text{ and } H = H_{\max}\,, \end{cases} \tag{11}$$

where

$$u_{\mathrm{d}} = \frac{1}{\tau_{\mathrm{d}} \cdot v^{\mathrm{r,i}}_{\mathrm{atp,g}}}\,.$$

Given that parameters $v_{\mathrm{max,up}}$, $v_{\mathrm{max,lo}}$, k_{atp} and k_{p}, which constitute the genotype of the cell, are proportional to the expression levels of glycolytic enzymes, we utilize these parameters to quantify the cost of expression, $v_{\mathrm{atp,e}}$. Because the expression costs of enzymes is difficult to estimate or measure experimentally [15], we chose to investigate two cost functions,

$$v_{\mathrm{atp,e}} = k_{\mathrm{e}}[(w_{\mathrm{up}} v_{\mathrm{max,up}})^n + (w_{\mathrm{lo}} v_{\mathrm{max,lo}})^n + (w_{\mathrm{atp}} c_{\mathrm{u}} k_{\mathrm{atp}})^n + (w_{\mathrm{p}} c_{\mathrm{u}} k_{\mathrm{p}})^n]\,, \tag{12}$$

$$v_{\mathrm{atp,e}} = k_{\mathrm{e}}[(w_{\mathrm{up}} v_{\mathrm{max,up}} + w_{\mathrm{lo}} v_{\mathrm{max,lo}} + w_{\mathrm{atp}} c_{\mathrm{u}} k_{\mathrm{atp}} + w_{\mathrm{p}} c_{\mathrm{u}} k_{\mathrm{p}})^n]\,, \tag{13}$$

Table 1. Parameter values used in the simulations.

Parameter	Value	Description
Extended core glycolysis model		
$v^{r}_{max,up}$	10 mM · min^{-1}	Maximal rate of upper glycolysis in the reference genotype [3]
$K_{M,glc}$	0.1 mM	Michaelis constant for glucose in upper glycolysis. Chosen to be approximately equal to $K_{M,glc}$ of hexokinase [11]
$K_{M,atp}$	0.1 mM	Michaelis constant for ATP in upper glycolysis [3]
$K_{i,atp}$	3 mM	Inhibitor constant for ATP in upper glycolysis [3]
a_{tot}	5 mM	Total concentration of ATP and ADP [3]
$v^{r}_{max,lo}$	10 mM · min^{-1}	Maximal rate of lower glycolysis in the reference genotype [3]
$K_{M,fbp}$	1 mM	Michaelis constant for FBP in lower glycolysis [3]
$K_{M,adp}$	0.1 mM	Michaelis constant for ADP in lower glycolysis [3]
$K_{M,p}$	2 mM	Michaelis constant for P_i in lower glycolysis [3]
k^{r}_{atp}	10 min^{-1}	ATPase reaction rate constant in the reference genotype [3]
k^{r}_{p}	0.3 min^{-1}	Rate constant of P_i import from the vacuole into the cytosol in the reference genotype [3]
$[P_i]_{vac,max}$	10 mM	Maximal concentration of P_i in the vacuole [3]
K_{vac}	250 mM	Size of the vacuolar phosphate store. Effectively, the capacity of the cell to accumulate FBP and other sugar phosphates. Not well known; value chosen to limit FBP to a few hundred mM [9]
m	4	Graduality of phosphate depletion from the vacuole
$[FBP]_0$	2 mM	Initial FBP concentration [3]
$[ATP]_0$	1 mM	Initial ATP concentration [3]
$[P_i]_0$	10.4 mM	Initial P_i concentration in the cytosol [3] used in all simulations except to determine B_g
	10 mM	Initial P_i concentration in the cytosol [3], used to determine B_g
Cell		
σ	0.1	Variation in the mutated value of a genotype parameter
μ	10^{-2}	Mutation rate of a genotype parameter
V_c	3.35×10^{-15} L	Cytosol volume of a spherical cell of diameter 2 μm with 20 % volume of organelles [20]
τ_g	90 min	Generation time of yeast [21]
τ_d	420 min	Death time of a yeast cell trapped in the imbalanced state. Estimated from ref. [3]
$v^{r,b}_{atp}$	12.7 mM · min^{-1}	ATPase flux of a cell with the reference genotype undergoing balanced glycolysis in an environment with constant 2 mM glucose. Estimated from ref. [3]
$v^{r,i}_{atp}$	0.46 mM · min^{-1}	ATPase flux of a cell with the reference genotype undergoing imbalanced glycolysis in an environment with constant 2 mM glucose. Estimated from ref. [3]
$v^{r}_{atp,e}$	5 mM · min^{-1}	Expression cost of the reference genotype
$v_{atp,m}$	0 mM · min^{-1}	General cell maintenance cost
Simulation		
N_0	50000	Initial population size in chemostat pre-simulation
	10000	Initial population size in the NCG scenario in pre-simulation
	12000	Initial population size in the two-genotype coexistence simulations
N^*	10000	Target population size
N_{tr}	100	Number of cells whose dynamics is tracked at any particular time
$V_{ch,0}$	1×10^{-8} L	Volume of chemostat chamber in pre-simulation
d_0	1×10^{-6} min^{-1}	Cell removal rate constant in NCG scenario in pre-simulation
D	5 min^{-1}	Dilution rate of the chemostat in the NCG scenario
t_s	0 min	Start of simulation time
t_{ms}	10000 min	Start of mutation-on segment
t_{me}	500000 min	End of mutation-on segment
t_e	800000 min	End of simulation time
Δt_p	5 min	Length of the integration interval during which the number of cells in the population does not change

(*Continued*)

Table 1. (Continued)

Parameter	Value	Description
Δt_s	1 min	Time interval at which the dynamics of metabolites, volume and health of tracked cells are saved for analysis
ODE solver		
$atol_c$	1×10^{-5} mM	Absolute tolerance for metabolite concentration
$rtol_c$	10^{-5}	Relative tolerance for metabolite concentration
$atol_v$	0.01×10^{-15} L	Absolute tolerance for cell volume
$rtol_v$	0	Relative tolerance for cell volume
$atol_h$	10^{-2}	Absolute tolerance for cell health
$rtol_h$	0	Relative tolerance for cell health

https://doi.org/10.1371/journal.pcbi.1008547.t001

where $c_u = 1$ mM is the unit concentration, introduced for dimensional consistency, w_{up}, w_{lo}, w_{atp}, w_p are weights of respective parameters on the total cost and k_e is a normalizing factor that assigns expression cost $v^r_{atp,e}$ to the reference genotype. Unless indicated otherwise, Eq 12 is used with $w_{up} = w_{lo} = w_{atp} = w_p = 1$ and $n = 4$, and Eq 13 is referred to as the alternative cost function. The rationale to consider similar weights for multi-step, multi-enzyme pathways of UG and LG, and single-protein ATP demand and phosphate transport reactions stems from the fact that a multi-step pathway can be sped up by increasing the rate of one rate-limiting reaction (e.g., hexokinase or phosphofructokinase in UG, or pyruvate kinase in LG [1, 16]). The nonlinearity in the cost function ensures that glucose flux through the pathway, and therefore ATP production, cannot be increased infinitely by the cell by increasing the total level of glycolytic enzyme expression.

Once the cell volume has increased to twice the standard cell volume V_c, the cell divides. To prevent clonal subpopulations from dividing or dying synchronously, we introduce individual variability in the initial cell volume and the parameter H_{max}. At the beginning of a simulation and after a cell division, each new (daughter) cell is assigned an individual uniformly distributed random value $H_{max} \sim U(0.9, 1.1)$; a new (daughter) cell always starts with $H = H_{max}$. Similarly, each new cell at the beginning of a simulation starts with initial uniformly distributed $V \sim U(0.5V_c, 1.5V_c)$, whereas after cell division, only one of the daughter cells is assigned such a random volume, while the other daughter cell is left with the volume complementary to $2V_c$, i.e., the volume of the parent cell is divided between the two daughter cells. A division event without mutation does not alter the metabolite, nor the enzyme concentrations in the daughter cells, consistent with a simple physical division. Daughter cells may be exposed to mutations of the genotype, which implies changing expression levels of corresponding glycolytic enzymes. Upon cell division, each parameter in the genotype of a daughter cell is modified with probability μ, or otherwise inherited from the mother cell. The modified value is drawn from a log-normal distribution

$$x_m = x_p e^X , \tag{14}$$

where x_p is the parental value, x_m is the mutated value in the daughter genotype and $X \sim N(0, \sigma^2)$ is a normally distributed random number with zero mean and standard deviation σ.

The final component of the model concerns the interaction between cells and the environment. A straightforward approach is to assume that the population of cells take up glucose, grow and divide in a chemostat chamber [17]. The glucose concentration in the chamber then

changes due to uptake by cells, inflow and outflow of the medium, such that

$$[\mathrm{Glc}]' = -\sum_i v_{\mathrm{up},i}\frac{V_i}{V_{\mathrm{ch}}} + D[\mathrm{Glc}]_0 - D[\mathrm{Glc}]\,, \tag{15}$$

where the sum is over all cells in the population, $v_{\mathrm{up,i}}$ is the upper glycolysis rate of cell i, V_{i} is the volume of cell i, V_{ch} is the volume of the chemostat chamber, $[\mathrm{Glc}]_0$ is the glucose concentration in the inflow medium and D is the dilution rate of the chemostat which is equal to F/V_{ch}, where F is the medium flow rate. Cells are washed out from the chamber at a rate N'_{out} proportional to population size N,

$$N'_{\mathrm{out}} = DN\,. \tag{16}$$

This is equivalent to cell removal rate per capita being independent of the population size and equal to D.

A chemostat is suitable to study a population of cells that compete for nutrient, because cells take up the nutrient and thus affect its concentration in the growth chamber. A mathematical analysis of the chemostat model shows that the nutrient concentration and the population size at steady-state depend on the maximum reproduction rate of cells [17]. Cells that reproduce faster, take up the nutrient faster, and thus, at steady-state, reach a larger population size and leave less nutrient in the growth chamber. As nutrient uptake and reproduction rates of cells evolve during evolutionary simulations, the steady-state nutrient concentration will also shift, making it difficult to determine the optimal evolutionary response of the metabolic pathway to a particular glucose availability regime. Therefore, we also considered an alternative model, where cell density is assumed to be so low that the consumption of glucose by cells has no noticeable effect on the glucose concentration in the chamber. In this version of the model, individual cell growth is still limited by glucose availability, but cells do not compete for glucose, i.e. population size is regulated by another mechanism, e.g., competition for limited space in a biofilm that is attached to the wall of the chamber [18]. We refer to such conditions as the NCG (No Competition for Glucose) scenario. The NCG conditions can arise as a limiting case of the chemostat model where cells are attached to the substratum in a large chamber with a high flow rate, i.e., where $V_{\mathrm{ch}} \to \infty$ and $F \to \infty$, while $D = F/V_{\mathrm{ch}}$ remains finite. The glucose uptake term in Eq 15 then vanishes and cells no longer affect glucose concentration in the chamber, i.e., $[\mathrm{Glc}] = [\mathrm{Glc}]_0$. However, glucose concentration in the chamber is still affected by the medium inflow and outflow, allowing us to impose a particular glucose dynamics regime by adjusting D and $[\mathrm{Glc}]_0$. In this alternative model, cell loss rate from the chamber is

$$N'_{\mathrm{out}} = dN^2\,, \tag{17}$$

where d is the removal rate constant. Here, in contrast to Eq 16, the per-capita cell loss rate increases with population size, reflecting the effect of competition for limited space.

Simulation procedure

The system of differential equations defined by Eqs 7, 10 and 11 for each cell, and by Eq 15 for the glucose dynamics in the chemostat chamber, was solved in intervals of Δt_{p} to obtain [FBP], [ATP], $[\mathrm{P_i}]$, V and H dynamics for each cell and [Glc] dynamics in the chemostat chamber. Integration was carried out with the Dormand-Prince fifth-order Runge-Kutta method [19] modified with a non-negativity constraint for the metabolite concentrations, i.e., if at the end of the integration step metabolite concentration c satisfied $-(\mathrm{atol_c} + |c|\mathrm{rtol_c}) < c < 0$, it was projected to zero. If after this procedure any other $c < 0$ remained, the integration step was

rejected and retried with a smaller step size. Between the integration intervals Δt_p, new cells are added to the population due to cell division, and cells are removed due to cell death and outflow from the chemostat.

A simulation was started with a population of N_0 cells. To ensure that initial cell genotypes were sufficiently fit to survive and reproduce in a given glucose regime, initial values of the evolving parameters of each cell were drawn from a uniform distribution $U(0.1P, 10P)$, where P is $v^r_{max,up}$, $v^r_{max,lo}$, k^r_{atp} or k^r_p respectively.

Simulation time was divided into three segments: (i) from simulation start time t_s to mutation start time t_{ms} the mutation process was disabled, allowing the establishment of a viable steady-state population from the genetic variation created at the start of the run; this was necessary because many initial random genotypes were not viable under a given glucose availability regime; (ii) from t_{ms} to mutation end time t_{me} cells were exposed to mutations enabling a gradual evolution of the metabolic pathway, (iii) from t_{me} to simulation end time t_e the mutation process was disabled once again to allow only the fittest genotypes to remain in the population. As the speed of evolution is expected to depend on the population size, we sought to normalize the equilibrium population size at the beginning of segment (ii) to be approximately N^* across all simulations. To achieve that, we first performed a pre-simulation without mutation of the same duration as segment (i) with provisional values that regulate population size, i.e. $V_{ch,0}$ for the standard chemostat model or d_0 for the NCG scenario. After determining the steady-state size population size N_p, full simulations with adjusted parameters $V_{ch} = V_{ch,0}\frac{N^*}{N_p}$ or $d = d_0\frac{N_p}{N^*}$ were run.

Data analysis

Throughout the simulation, we tracked and saved the metabolite, volume and health dynamics of a randomly selected subpopulation of N_{tr} cells at time intervals of Δt_s. From this data, we find the fractional volume increase rate of tracked cells, V'/V, which is equivalent to the cell reproduction rate r in population dynamics models. We also define an indicator to quantify the balancedness of the dynamics of the model glycolysis pathway in a fluctuating environment. In a balanced cell, high external glucose coincides with high intracellular ATP, whereas in an imbalanced cell, high external glucose coincides with low intracellular ATP. The phenotypic balancedness of a cell, $B_{p,cov}$ is therefore defined as covariance between the external glucose concentration and intracellular ATP concentration during an integral number of cycles in a periodic environment where the cell lives,

$$B_{p,cov} = \mathrm{cov}([\mathrm{Glc}], [\mathrm{ATP}])\,. \tag{18}$$

$B_{p,cov}$ will have positive values if the dynamics of glycolysis is balanced and negative values if it is imbalanced. This measure is appropriate if glucose and ATP values oscillate regularly around their means; it is more difficult to interpret when the dynamics is irregular, as in the case of catastrophic dynamics (see Section *Evolution of increased imbalancedness*. . . below).

Under the NCG scenario studied here, the external glucose concentration in the chamber changes abruptly between a high value during the ON phase and a low value during the OFF phase because of a high dilution rate (D). Therefore, a simpler and more easily interpretable measure of phenotypic balancedness, $B_{p,phs}$, can be used by comparing the average ATP concentrations in the cell during ON and OFF phases:

$$B_{p,phs} = [\mathrm{ATP}]_{on} - [\mathrm{ATP}]_{off}\,. \tag{19}$$

Also here, positive values indicate balanced dynamics (more ATP is produced and a cell grows faster during the ON phase), whereas negative values indicate imbalanced dynamics (more ATP is produced and a cell grows faster during the OFF phase).

Balanced and imbalanced glycolysis can exist as alternative steady-states for the same genotype. Therefore, we define the balancedness of a genotype (B_g) as its propensity to exhibit balanced dynamics. Genotypic balancedness is determined by the following procedure, in part similar to the one described by van Heerden at al. [3] For each genotype, we generate 100 random initial metabolite concentrations, apply a particular glucose concentration and simulate the metabolite dynamics for 300 min. The initial metabolite concentrations are normally distributed with either realistic constant means for all cells, $[FBP]_0$, $[ATP]_0$, $[P_i]_0$ ($B_{g,1}$) or, in case of constant external glucose in NCG scenario, also the actual metabolite concentrations in evolved cells ($B_{g,2}$), and realistic variation, CV = 6 %. We repeat the procedure for a range of glucose values, 2.00 mM, 1.95 mM, . . ., 0.05mM. $B_{g,1}$ or $B_{g.2}$ is then the largest concentration of glucose that results in a balanced metabolism for all 100 random initial metabolite concentrations, or 0 mM otherwise. Thus, higher B_g indicates a more balanced genotype. To determine whether the metabolism is balanced or not in each of these simulations, we apply the following criterion. In a balanced phenotype under constant [Glc], [FBP] reaches a steady-state value. Eq 7 shows that at the steady-state

$$v_{up} = v_{lo} + [FBP]\frac{V'}{V}\,. \tag{20}$$

Taking into account that the cell needs time to reach metabolic steady state, the phenotype is considered balanced if Eq 20 holds true within 0.1% relative error for more than 10% of the simulation time.

Results

We first investigate the evolution of the core glycolysis pathway in an environment with a constant concentration of glucose (NCG scenario, see Model and methods). In each of these simulations, the pathway evolves to optimize its performance in the particular glucose availability regime that is imposed externally. Next, we consider the evolution of the pathway in populations subject to competition for glucose in a chemostat, where adaptation of the pathway alters the ecological conditions experienced by the population. Due to this eco-evolutionary feedback, no single strategy may be optimal in a given environment, creating the possibility of more complex eco-evolutionary dynamics.

Pathway adapted to scarce glucose exhibits imbalanced dynamics under ample glucose

Under NCG conditions, the core glycolysis pathway adapts to different constant levels of glucose availability by optimizing the expression levels of glycolytic enzymes (Fig 2A). The evolved expression pattern optimizes the balance between three selective forces. One component of selection favors an increase in $v_{max,up}$, $v_{max,lo}$ and k_{atp}, because the increasing flux of glucose through the pathway enhances ATP production and cell growth rate. Next, there is a pressure to lower these genotype parameters in order to reduce the cost of expression. Finally, selection acts against $v_{max,up}$ becoming too large compared to $v_{max,lo}$ to avoid the loss of fitness due to cells falling into the imbalanced state.

When comparing optimal expression patterns between environments, we observe that pathways evolve to increase the difference $v_{max,up}-v_{max,lo}$ as glucose concentration decreases (Fig 2A). Because at low glucose concentration the risk for a cell to become imbalanced is low,

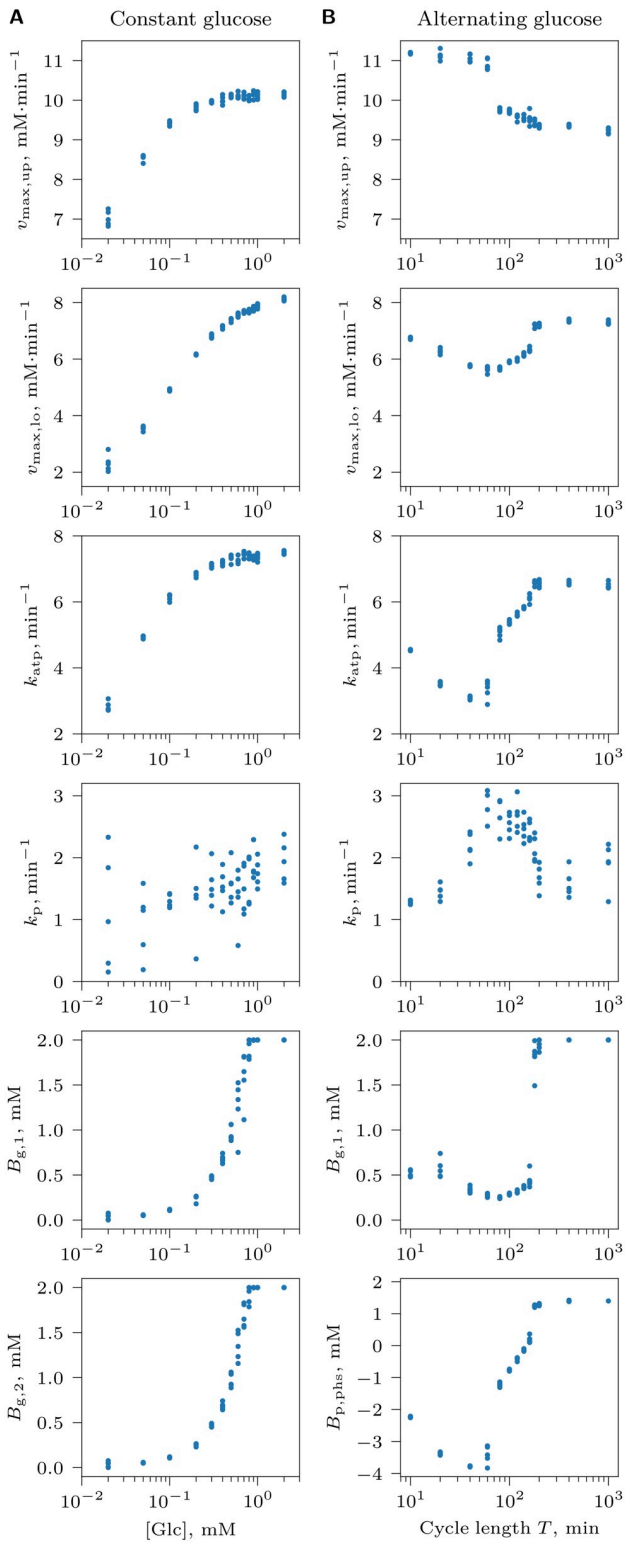

Fig 2. Optimization of the core glycolysis pathway in the absence of competition for glucose under NCG conditions with (A) a constant glucose supply concentration $[Glc]_0$, or (B) an alternating glucose availability consisting of ON ($[Glc]_0 = 2$ mM) and OFF ($[Glc]_0 = 0.01$mM) phases of equal duration with period $T = T_{on} + T_{off}$. Each dot represents the average of an evolving genotype parameter ($v_{max,up}$, $v_{max,lo}$, k_{atp} and k_p) or a measure of balancedness at the end of an evolutionary simulation (t_e). Genotype parameter averages were computed over the entire population of cells;

balancedness values $B_{g,1}$, $B_{g,2}$ were averaged over a randomly selected subpopulation of cells that were tracked individually, and $B_{p,phs}$ was calculated for the subset of tracked cells that survived through at least one ON and one OFF phase. Results of 5 replicate simulations are shown for each of the studied [Glc] and T value.

https://doi.org/10.1371/journal.pcbi.1008547.g002

and because the costs of UG and LG are comparable ($w_{up} = w_{lo} = 1$), cells evolve higher $\nu_{max,up}$ at the expense of $\nu_{max,lo}$ to increase glucose uptake and thus gain a competitive advantage. As a consequence, these cells become more vulnerable to imbalanced dynamics at high glucose concentration (Fig 2A, $B_{g,1}$ and $B_{g,2}$). Throughout, we observe low values of k_p and a relatively high level of variation in this parameter, indicating that k_p is under weak selection. Since cells at constant glucose must show a balanced phenotype to survive, and phosphate transport is of little importance for balanced cells, k_p likely evolves to low values solely in response to weak selection for a reduction in the cost of enzyme expression.

Results are qualitatively similar when the cost of LG is much larger than that of UG ($w_{up} = 0.1$, $w_{lo} = 1$). In this case, high expression of UG enzymes can evolve to enhance glucose uptake at low glucose without major costs to the cell, while the expression of LG enzymes cannot be increased to the same level without the cell incurring prohibitive costs. By contrast, when the cost of LG is much lower than that of UG ($w_{up} = 1$, $w_{lo} = 0.1$), LG evolves high expression levels matched with the rate of UG, so that the evolved cells are balanced under any glucose concentration (S2 Fig).

Imbalanced dynamics shows fitness advantage over balanced dynamics at quickly varying glucose

Next, we studied the adaptation of the pathway to a fluctuating NCG environment with alternating $[Glc]_0 = 2$ mM ON and $[Glc]_0 = 0.01$ mM OFF phases of equal duration. Interestingly, cells of various balancedness coexisted in the population to form a continuum of strategies of nearly identical fitness, from strongly balanced to strongly imbalanced (Figs 3 and 4 at time t_{me}, and S1–S3 Videos). The two extremes of this balancedness continuum illustrates two radically different strategies of survival under varying glucose. Upon sudden glucose availability during the ON phase, balanced cells (BCs) immediately start maintaining high ATP levels and grow, and continue to do so until the ON phase is over (Fig 3A). In contrast, imbalanced, "greedy" cells (ICs) do not immediately elevate ATP level, but channel all produced ATP to accumulate FBP as intracellular storage that is used up during the OFF phase to maintain a high level of ATP needed for growth (Fig 3C). The polymorphism in the population was only observed during the mutation-on segment of the simulation (i.e. between times t_{ms} and t_{me}), indicating that it was caused by mutation-selection balance, a dynamic steady-state in which inferior mutants are created at the same rate as they are purged from the population by selection [22]. After mutations were stopped, only one strategy with the highest fitness survived at the final time point (Fig 4, time t_e).

The optimal strategy depended on the period of glucose fluctuations T (where $T = T_{on} + T_{off}$): ICs survived at quickly varying glucose (Fig 4, $T = 40$ min and S1 Video), whereas BCs were favored when environmental fluctuations were slow (Fig 4, $T = 200$ min and S3 Video). Periods of intermediate lengths resulted in strategies that were neither strongly balanced nor imbalanced (Fig 4, $T = 120$ min, Fig 3B and S2 Video). This dependency is reflected in the evolved genotypes: the difference $\nu_{max,up} - \nu_{max,lo}$ is large for short cycles, and small for long cycles, a feature of imbalanced and balanced genotypes respectively (Fig 2B). Evolved k_p values have smaller variation than at constant glucose and are largest at cycle lengths with the most strongly imbalanced cells (Fig 2B). This is consistent with a selective pressure to keep phosphate transport at an optimal level, because it plays a crucial role for FBP accumulation in ICs.

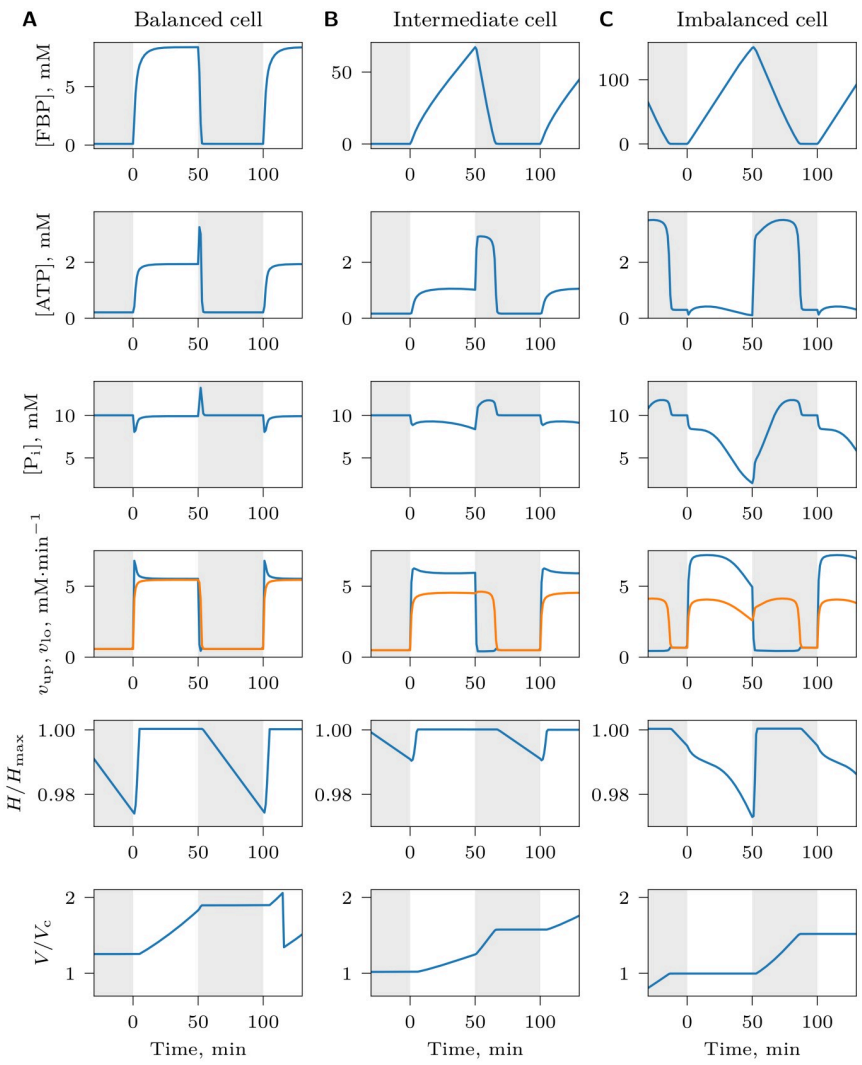

Fig 3. Metabolite and growth dynamics of individual cells under NCG conditions with an alternating high and low supply of glucose. Dynamics of (A) a balanced cell, $B_{p,phs}$ = 1.45 mM, (B) a cell that is neither strongly balanced nor strongly imbalanced, $B_{p,phs}$ = −0.03 mM, and (C) an imbalanced cell, $B_{p,phs}$ = −2.13 mM. Regions with white and gray background indicate alternating glucose supply ON phase ($[Glc]_0$ = 2mM) and OFF phase ($[Glc]_0$ = 0.01mM), respectively. In the v_{up}, v_{lo} plot, v_{up} is shown in blue and v_{lo} in orange. Time is shown relative to the beginning of a ON-OFF cycle. Note the different scales of FBP dynamics in (A), (B) and (C). In (A), a sudden drop in V/V_c indicates a cell division.

https://doi.org/10.1371/journal.pcbi.1008547.g003

Why does the optimal strategy in a periodically fluctuating environment depend on the cycle length T? ICs would be expected to have higher fitness than BCs irrespective of how rapidly glucose fluctuates, because they could sustain larger $v_{max,up}$ at the expense of $v_{max,lo}$, and thus would be able to take up glucose faster than BCs. Consistent with this idea, ICs that evolved at short cycles indeed take up glucose faster than BCs that evolved at long cycles, and therefore have higher v_{atp} flux (S4 Fig). One obvious explanation of the success of BCs in slowly varying environments could be that FBP accumulates to high concentrations in the cytosol of ICs during long ON phases, depleting phosphate reserves from the vacuole. As a result, subsequent accumulation of FBP becomes less efficient, limiting the potential of growth of ICs. FBP accumulation does indeed slow down with increasing FBP in the cytosol (see

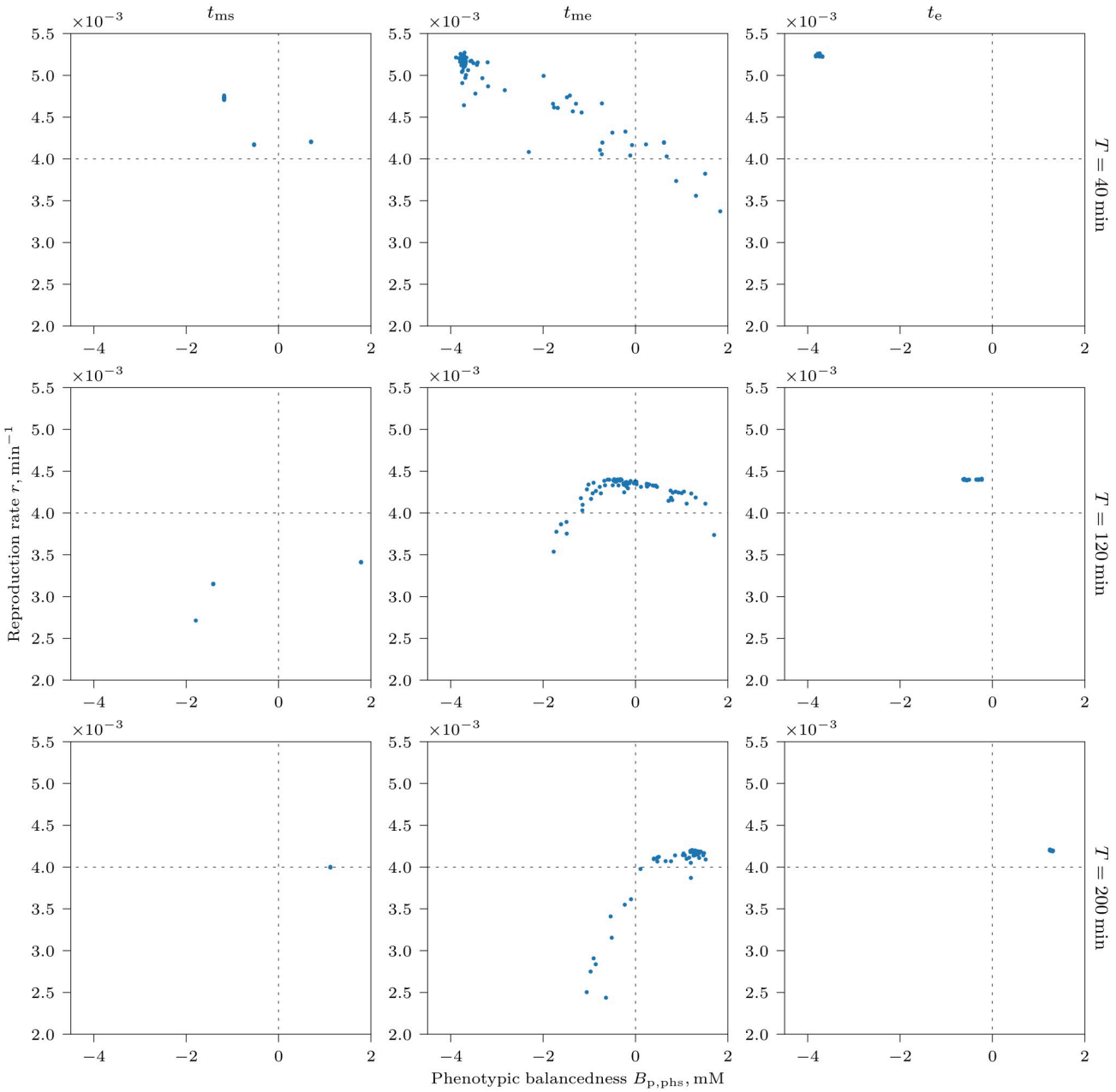

Fig 4. Average reproduction rate *r* of tracked cells during an environmental cycle (ON and OFF phase), plotted against their phenotypic balancedness $B_{p,phs}$ at different times (t_{ms}, t_{me} and t_e, columns) in the NCG scenario with alternating glucose supply for different glucose cycle length *T* (rows). Points right of vertical dashed line ($B_{p,phs} > 0$) indicate balanced cells, whereas points left of the line ($B_{p,phs} < 0$) indicate imbalanced cells. The mutation-on segment of the simulation starts at time t_{ms} with surviving genotypes sampled from random standing genetic variation introduced at the beginning of the simulation. Mutations with small phenotypic effects then allow for a gradual evolution of the reaction rates between times t_{ms} and t_{me}. Mutation is switched off again during the final segment of the simulation (between t_{me} and t_e) so as to allow suboptimal genotypes to be purged from the population. Points with higher *r* values reflect higher cell growth rates; cells with the highest *r* values at time t_{ms} are the ones to survive at the end of the simulation (time t_e). Therefore, *r* appears to be a good proxy for cell fitness (i.e., reproduction rate *r* minus death/removal rate), indicating that cells of different strategies do not differ markedly in removal and death rate. S1–S3 Videos show the dynamics of these plots during the whole length of simulation.

https://doi.org/10.1371/journal.pcbi.1008547.g004

Section *Evolution of increased imbalancedness*. . . below), but further analysis shows that this effect is not solely responsible for the fact that BCs outcompete ICs in slowly varying environments. In particular, if we allow the pathway to evolve without phosphate depletion in the vacuole ($K_{vac} \to \infty$), we still observe the same evolutionary outcome. BCs also outcompete ICs if the cost of phosphate transport is reduced by an order of magnitude ($w_p = 0.1$), if cell health does not deteriorate ($t_d \to \infty$) or if a different expression cost function is used (Eq 13, S3 Fig). Instead, the advantage of BCs during long cycles arises because the glucose uptake rate per cell is proportional to cell volume, which changes differently through time for the two cell types. BCs increase in size as they take up glucose, leading to an acceleration of glucose uptake during the ON phase. By contrast, ICs take up glucose without increasing in size during during the ON phase, leading to a constant glucose uptake rate. Thus, as the cycle length increases, the uptake rate of BCs eventually outpaces that of ICs (S1 Text and S1 Fig). This effect can be seen in Fig 4, where at $T = 40$ min, the growth rate of ICs is higher than that of BCs, but the situation is opposite at $T = 200$ min.

Interestingly, cell balancedness also slightly increases in rapidly fluctuating environments (very small T, Fig 2B). This suggests that another selective pressure on ICs plays a role: although an increase in $v_{max,up}$ at the expense of $v_{max,lo}$ will enhance glucose uptake rate and give a competitive advantage to cells, $v_{max,lo}$ still has to be fast enough for all FBP accumulated during the ON phase to be fully used up during the OFF phase. This challenge becomes more difficult as the glucose cycle becomes shorter. Indeed, the cycle length below which cell balancedness slightly increases ($T \approx 60$ min) corresponds to the point where the FBP usage time during the OFF phase approaches the length of the OFF phase (S4 Fig).

One potential complication in interpreting our results is possible phenotype switching in cells with similar genotypes. In the absence of mutation, cell division does not perturb metabolite equilibria in daughter cells (Eq 7). However, a mutation upon cell division can trigger the switch of metabolic balancedness to a different state in the daughter cell, even though its genotypic balancedness is similar to that of the parent cell. We compared the genotypic and phenotypic balancedness ($B_{g,1}$ and $B_{p,phs}$) of the evolved cells and found that they are well correlated (Fig 2B). This indicates that phenotype is largely determined by the genotype in our simulations and that phenotypic variation among genetically nearly identical cells is minimal.

Competition for glucose can give rise to stable coexistence of balanced and imbalanced cells

After characterizing the optimization of the glycolytic pathway in response to different externally imposed glucose availability regimes (NCG conditions), we next considered the evolution of the pathway under chemostat conditions. Here, cells compete for glucose and its availability changes in response to the evolving utilization strategy of the population. As a result of this feedback between evolutionary and ecological factors, selection may no longer lead to a single optimal genotype [23].

The simulated input into the chemostat was a pulse train of glucose, consisting of a short $T_{on} = 1$ min ON phase of $[Glc_0] = 300$ mM that resulted in a sharp increase in glucose in the chamber up to a few mM, followed by a longer OFF phase (either of constant or variable length) with a minimal glucose supply $[Glc_0] = 0.01$ mM, during which the glucose concentration in the chamber decreased due to outflow and uptake by cells. As in our earlier simulations, we observed that short and long environmental cycles favored ICs and BCs respectively (S5 and S7 Figs). However, intermediate cycle lengths T and dilution rates D often resulted in stable coexistence of BCs and ICs in the population (Fig 5, S6 and S8 Figs). Contrary to what was observed in the NCG simulations, the dimorphism in the chemostat conditions did not rely on

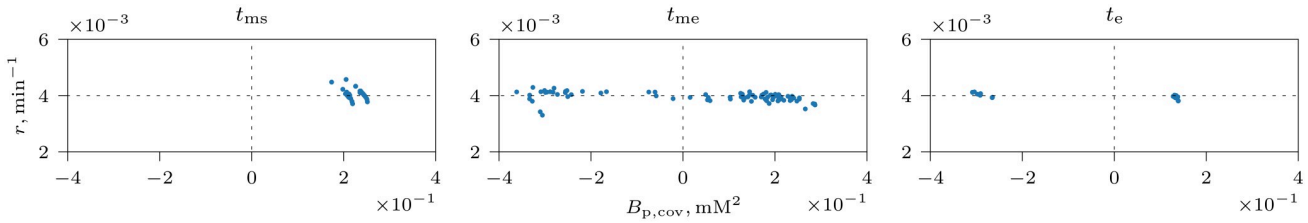

Fig 5. Evolution of a dimorphic population. Each dot represents the reproduction rate r of a tracked cell averaged over an environmental cycle plotted against its phenotypic balancedness $B_{p,cov}$. Data are shown for three time points during a simulation in a chemostat with a variable OFF phase, $\overline{T} = 100$ min, $T_{on} = 1$ min, $\overline{T}_{off} = 99$ min, CV(T_{off}) = 5 %, and $D = 4 \times 10^{-3}$ min^{-1}. The initial balanced population (left, time t_{ms}) accumulates variation created by mutation (middle, time t_{me}). At the end of the simulation (t_e), subpopulations of BCs and ICs coexist at a stable equilibrium frequency. S4 Video shows the dynamics of this plot during the whole length of the simulation.

https://doi.org/10.1371/journal.pcbi.1008547.g005

a continuous generation of new mutants, i.e., the polymorphism was stable at the end of the mutation-off segment of the simulation, indicating that it was not supported merely by mutation-selection balance. Instead, diversity was maintained by negative frequency-dependent selection, whereby two strategies can stably coexist if the fitness of each is greater when rare, a phenomenon known as protected polymorphism [22].

Negative frequency dependence occurs when each strategy competes more strongly with cells of the same type than with the ones utilizing the other strategy. To demonstrate that this phenomenon is responsible for the observed coexistence, we randomly picked two genotypes from BC and IC subpopulations at the end of the simulation (shown in Fig 5, time t_e, Table 2), constructed mixed populations with a range of initial fractions of BCs, f_b, and ICs, $1-f_b$, and then simulated their joint population dynamics in the absence of mutation. For all initial f_b values, populations restored the same equilibrium frequency of BCs (Fig 6A), except in a few cases where a high fraction of ICs (low f_b) caused catastrophic dynamics and ICs were wiped out, seen as a sudden jump in f_b value to 1 (see Section *Evolution of increased imbalancedness*. . . below). Consistent with this evidence, the reproduction rates of ICs and BCs were observed to decrease as their fractions in the population increased (Fig 6B). Reproduction rate is a good proxy for cell fitness in our simulations, because cells rarely die and are removed from the chemostat mostly by outflow with constant removal rate per cell D that is independent of cell strategy (Eq 16).

Frequency dependence in the chemostat arises because a population dominated by BCs (BCP) affects the profile of glucose concentration dynamics in the chemostat chamber differently than a population dominated by ICs (ICP) (Fig 6D(i)). As a result, glucose uptake, ATP production and the growth dynamics of the two types of cells are differentially affected in the two types of populations, such that each strategy enjoys an advantage of being rare (Fig 6D(ii) and 6D(iii)). The fitness advantage of rarity can be quantified by comparing the glucose consumption by a cell over an environmental cycle when its cell type is rare in the population

Table 2. Genotypes used in no-mutation coexistence simulations. Also indicated are the expression costs of the genotypes.

	BC	IC
$v_{max,up}$	9.90956 mM · min^{-1}	10.92211 mM · min^{-1}
$v_{max,lo}$	6.97388 mM · min^{-1}	5.65143 mM · min^{-1}
k_{atp}	6.14105 min^{-1}	4.82003 min^{-1}
k_p	1.27357 min^{-1}	2.07099 min^{-1}
$v_{atp,e}$	2.24 mM · min^{-1}	2.63 mM · min^{-1}

https://doi.org/10.1371/journal.pcbi.1008547.t002

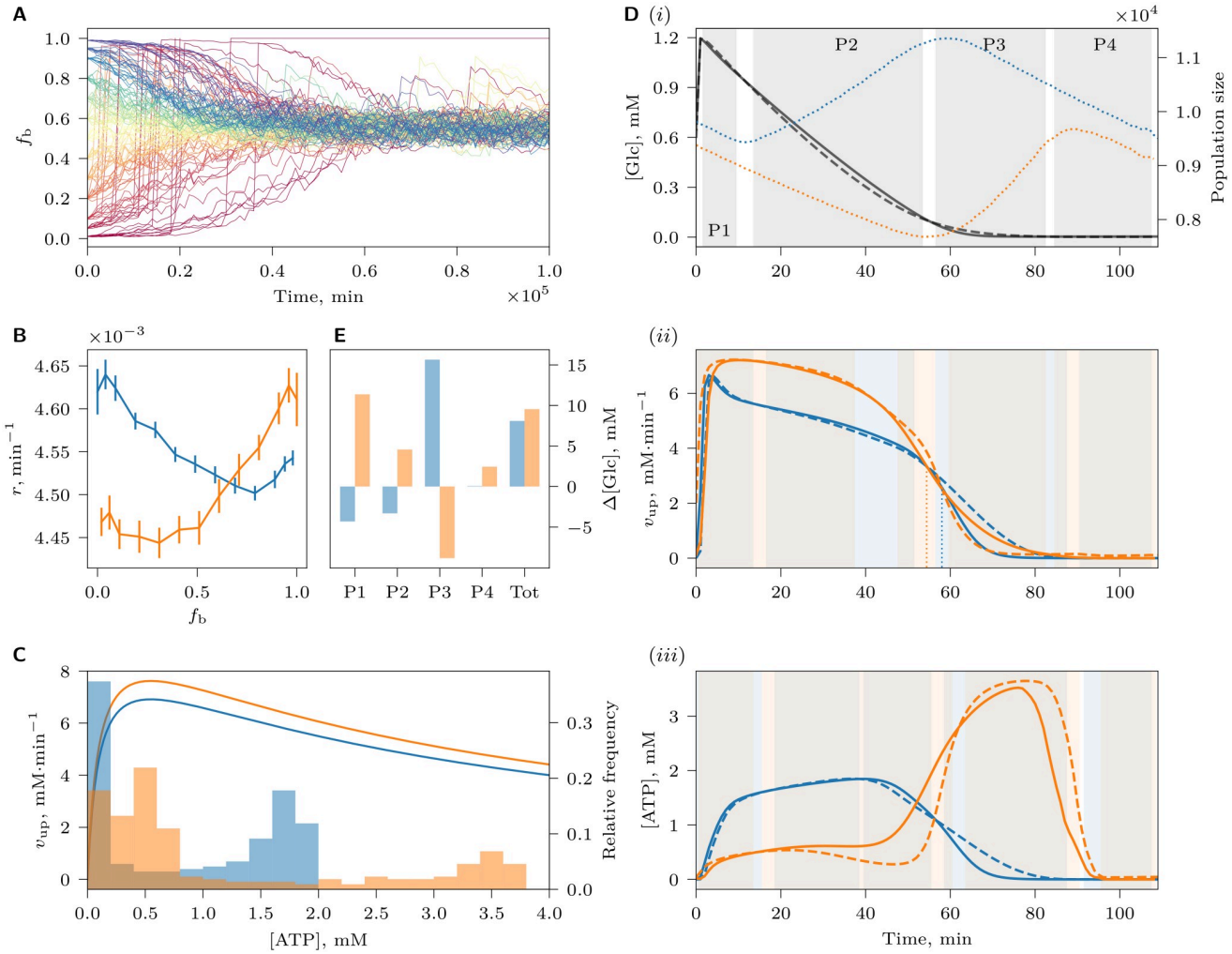

Fig 6. Negative frequency-dependence maintaining coexistence between BCs and ICs. (A) The joint population dynamics of two genotypes (Table 2), picked from the BC and IC subpopulations of the dimorphic population shown in Fig 5, was simulated under chemostat conditions as in Fig 5, but without mutation. Trajectories show the fraction of BCs (f_b) in the population over time, for multiple different initial values of f_b, indicated by color. In B, C, D(ii), D(iii) and E, data for BCs and ICs are shown in blue and orange, respectively. (B) Reproduction rate of BCs and ICs as a function of their fractions in the population. Error bars indicate confidence intervals ($\alpha = 0.05$) of the mean of the reproduction rates across simulation replicas. (C) Rate of UG, v_{up} (lines, left axis), as a function of intracellular ATP concentration (Eq 1) for BCs and ICs at [Glc] = 2mM. Histograms (right axis) show the relative frequency distribution of intracellular ATP concentration values in BCs and ICs during an environmental cycle (shown in D(iii)). (D) Average glucose, v_{up} and ATP dynamics during an environmental cycle (horizontal axis measures the time since the start of the glucose pulse) for a cell in a BCP ($f_b = 0.99$) or ICP ($f_b = 0.01$). (i) Average glucose concentration profile (left axis) in the chemostat chamber during an environmental cycle in a BCP (solid line) and an ICP (dashed line). Gray background indicates phases P1-P4 that are defined by a significant difference in the average glucose concentration between BCP and ICP ($\alpha = 0.05$, Bonferroni adjusted). Blue and orange dotted lines indicate average population sizes of BCP and ICP respectively (right axis). Due to the difference in the timing of reproduction of BCs and ICs, BCP and ICP show different size dynamics: BCP increases in size during the first half of the cycle when BCs reproduce, and decreases in size when reproduction stops and cells are only removed from the chemostat by the outflow. Conversely, ICP increases in size in the second half of the cycle, when ICs reproduce. (ii) Average v_{up} and (iii) ATP dynamics during an environmental cycle, when the focal cell type is the dominant type (solid line) or the rare type (dashed line) in the population. Because the expression cost of an IC is higher than that of a BC (Table 2), an IC has to take up more glucose than a BC to maintain the same growth rate. Blue (resp., orange) background indicates phases where the averages shown by blue (resp., orange) curves differ significantly; gray background highlights phases where both differ within each pair. Dotted lines in (ii) indicate time points when glucose uptake flux v_{up} in BCs and ICs becomes equal (in ICP, orange dotted line; in BCP, blue dotted line). (E) Advantage of rarity measured as the differential glucose uptake per unit cell volume, Δ[Glc], compared between populations where the focal cell type is rare versus dominant. Data are shown integrated over the entire environmental cycle (Tot), as well as separately for the phases P1-P4 (here, these include both shaded areas in D(i) and half of the adjacent white space between them). Due to demographic stochasticity, estimates in (B) and (D) were obtained by averaging over many environmental cycles after [Glc] in the chemostat had reached equilibrium and where f_b had not deviated markedly from the considered value.

https://doi.org/10.1371/journal.pcbi.1008547.g006

relative to when it is dominant. This difference in glucose consumption, Δ[Glc], is proportional to the differential ATP production by the strategy and thus translates directly into a difference in reproduction rate and fitness. In Fig 6E, we show Δ[Glc] over four phases of the environmental cycle (P1-P4); these phases, defined merely for easier reference to the phenomena occurring during the environmental cycle, were identified by a significantly different average concentrations of glucose in the chemostat chamber between BCPs and ICPs. We first observe that whenever one of the two cell types profits from being rare, the other suffers a disadvantage of rarity. Further, BCs are the superior competitor during the P3 interval of the environmental cycle, whereas ICs are the superior competitor during intervals P1, P2 and P4. The positive fitness effects of rarity, however, outweigh the negative effects for both cell types when averaged over the entire environmental cycle, creating the necessary conditions for stable coexistence by negative frequency dependence. It should be noted that the glucose consumption differences and the resulting frequency-dependent fitness effects are rather subtle for each of the two cell types, ≈ 3 %. However, fitness differences of such magnitude can have substantial effects over evolutionary time. For example, a strategy with a competitive advantage of 3 % is expected to spread to fixation on a time scale of $4/(3\ \%) \approx 133$ generations (based on the rate of spread of a beneficial allele with frequency 0.5 and fitness advantage s = 0.03). This estimate corresponds well with the time scale for convergence to equilibrium in Fig 6A: for a reproduction rate observed in the simulations (Fig 4), 133 generations/4.5×10^{-3} generations · $\text{min}^{-1} \approx 0.3 \times 10^5$ min.

In the remaining part of this section, we provide a detailed account of the mechanisms responsible for generating negative frequency dependence, intended for interested specialist readers. Others may skip this text and proceed to the next section. At the root of the observed frequency dependence is a feature of the core glycolysis pathway whereby the rate of UG is inhibited by high concentrations of ATP, so that v_{up} reaches a maximum value at an intermediate ATP concentration (Eq 1, Fig 6C). As a result, cells face a trade-off between high ATP concentration, and thus high growth rate, and fast glucose uptake. Further, it should be noted that because ICs evolved a higher expression level of UG enzymes than BCs in our simulations (Table 2, also see S4 Fig), the UG rate of the IC lies above that of the BC for all ATP concentrations (Fig 6C). An additional difference between the cell types reveals itself when we compare the actual ATP concentrations that occur in BCs and ICs during an environmental cycle (blue and orange histograms; Fig 6C): where BCs operate under a regime of intermediate ATP concentrations that appears to reflect a compromise between maintaining high ATP and achieving a high rate of UG, ICs can be clearly seen to switch between two different modes of operation, one maximizing v_{up}, the other yielding a high ATP concentration. The first mode, which is characteristic of the imbalanced state, gives an extra boost to the competitive advantage of ICs at the start of the environmental cycle, when glucose is available at high concentration. However, when glucose becomes scarce at the gradual onset of starvation, ICs switch to their second mode of operation, producing high intracellular ATP concentrations from accumulated FBP. As a result, the flux through upper glycolysis shuts down abruptly in ICs, leaving most of the remaining glucose to be consumed by BCs. Since the two types of cell are more efficient in glucose uptake at different times, each type will compete more with the same than with another type, which leads to negative frequency dependence of fitness.

Fig 6D explains how this phenomenon in turn leads to the advantage of rarity for ICs and BCs during intervals P2 and P3 respectively. Let us first focus on why ICs (orange lines in D(ii) and (iii)) do relatively better in a BCP (dashed orange) than in a population dominated by their own type (ICP; solid orange) during interval P2. It should be first noted that glucose dynamics in the chemostat chamber is determined by the glucose uptake rate of the dominant cell type, as well as the size of its population. Since ICs during interval P2 are in the low ATP,

efficient glucose uptake mode, BCP consumes the available glucose somewhat slower than ICP in the first half of P2 (Fig 6D(i), P2), allowing ICs to maintain the imbalanced metabolic state for a slightly longer period of time (≈ 5 min, Fig 6D(ii), dotted lines). As a result, the decrease of ν_{up} at the onset of starvation is delayed (Fig 6D(ii)), and low ATP concentration (characteristic of metabolic imbalance) persists for a longer period of time, so that the cell can accumulate more FBP and ultimately produce more ATP during the OFF phase (Fig 6D(iii)). (Note that glucose consumption of ICP ultimately slows down in the second half of P2, because it also depends on the ICP size, which decreases during P2, as ICs do not divide and are only removed from the population by outflow (Fig 6D(i), orange dotted line); glucose concentration therefore equalizes between BCP and ICP at the end of P2). After the switch of ICs to high ATP, slow glucose uptake mode as glucose concentration decreases in interval P3, BCs become more efficient in glucose uptake, and therefore BCP reduces the glucose concentration faster than ICP. As a result, BCs (blue lines in Fig 6D(ii) and 6(iii)) do better when they are rare in a population dominated by ICs (dashed lines): the remaining glucose is only very slowly consumed by ICs, but is mostly taken up by BCs. By contrast, in a BCP (solid lines), BCs compete for glucose with other cells of the same type right until little glucose is left.

The advantage of rarity of ICs during intervals P1 and P4 manifests itself through a different mechanism. At the end of the cycle (during P4), glucose concentration in the environment is very low, and ICs have already used up all their FBP. As a result, ATP concentration in both cell types is very low. Because ICs in this state take up the remaining scraps of glucose a little faster than BCs (ν_{up} is higher for ICs close to the point [ATP] = 0, Fig 6D), ICs in BCP enjoy a slightly larger glucose concentration, and therefore a slightly larger ATP concentration, leading to the advantage of rarity. Due to the autocatalytic nature of the glycolytic pathway (i.e., the pathway needs ATP investment to generate more ATP), this will allow ICs in BCP to restart glucose uptake slightly faster upon glucose availability at the beginning of the next cycle (P1), giving them a fitness advantage.

Evolution of increased imbalancedness renders populations vulnerable to catastrophic collapse

Evolved populations transitioned from being dominated by BCs to being dominated by ICs at intermediate values of environmental cycle length (T) and chemostat dilution rate (D) (S5–S8 Figs). Here, populations were often observed to exhibit catastrophic events whereby population size collapsed and then recovered (Fig 7A and 7B, also Fig 6A). Interestingly, during a catastrophe, the fraction of ICs in the population drops and BCs become dominant, but in-between two adjacent catastrophic events, the fraction of ICs increases as they are more competitive than BCs (Fig 7B and S11 Fig). These eco-evolutionary cycles result from a vulnerability of ICPs: a stochastic decrease in the population size can temporarily elevate the concentration of glucose in the chemostat (see Model and methods), forcing ICs to spend more time in the imbalanced state accumulating FBP and less time processing FBP to maintain high ATP needed for reproduction. As a result, FBP increasingly accumulates in ICs over many environmental cycles because it cannot be fully processed, and the reproduction rate of ICs decreases (Fig 7B), leading to a further decrease in the population size and elevation of the glucose level. In ICPs with strongly ICs that are particularly prone to accumulate more FBP than they can handle, this positive feedback can easily escalate into a catastrophic collapse of the population, where most of the ICs are lost. When such a catastrophe occurs, the population can survive if it still contains a small subpopulation of BCs that survived the competition with ICs. BCs profit from the increased glucose concentration by reproducing faster, causing the population size and the glucose concentration to be restored to their normal levels. The

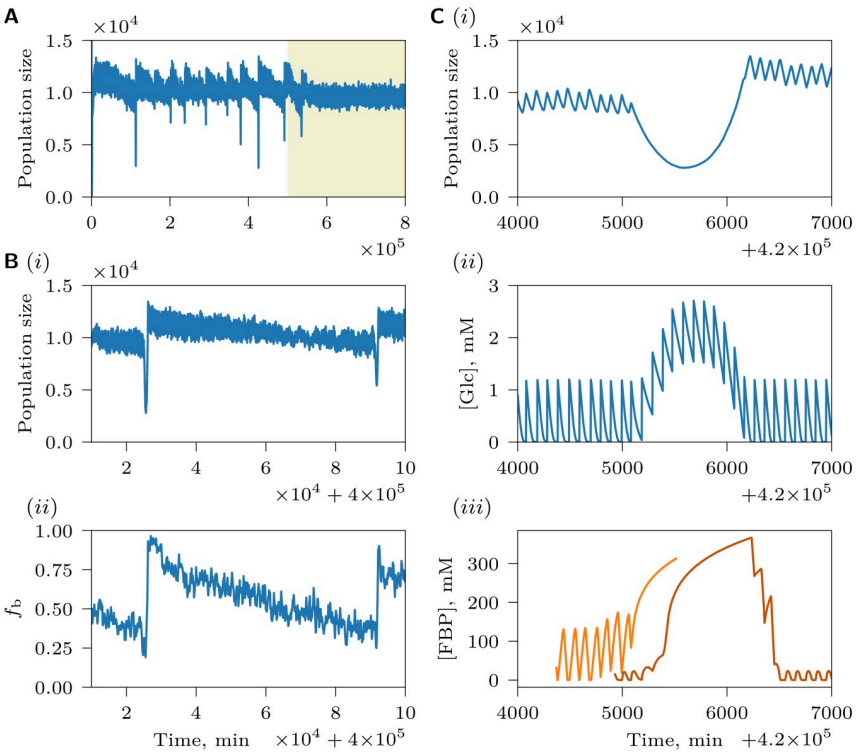

Fig 7. Catastrophic dynamics of the population shown in Fig 5. (A) Population size during the whole length of the simulation. Yellow background indicates the mutation-off segment of the simulation. (B) (i) Population size between two catastrophic events and (ii) the corresponding fraction of BCs of tracked cells, f_b, where a BC is defined as having a positive phenotypic balancedness $B_{p,cov}$. An apparently decreasing population size between catastrophic events shown in (A) and (B)(i) is due to the difference in the timing of reproduction of BCs and ICs (Fig 6D(i)). Just after the catastrophe, the population is dominated by BCs and therefore population reaches larger sizes than immediately before the catastrophic event, when the population is dominated by ICs. (C) A close-up of a catastrophe: (i) population size, (ii) glucose dynamics and (iii) FBP dynamics of two example cells, strongly imbalanced ($B_{g,1}$ = 0.15 mM, light orange) and weakly imbalanced ($B_{g,1}$ = 0.55 mM, dark orange). The strongly imbalanced cell begins accumulating large amounts of FBP earlier than the weakly imbalanced cell. One cell is removed by outflow in the middle of the catastrophic event, whereas the other survives the catastrophe and recovers.

https://doi.org/10.1371/journal.pcbi.1008547.g007

surviving population is dominated by BCs, which, however, create ideal conditions for more competitive imbalanced strategies to evolve. ICs, either the ones that survived the catastrophe, or newly generated mutants, will therefore increase in frequency and evolve to become more imbalanced (i.e. competitive) over time, causing the cycle to repeat. Catastrophic dynamics thus depends on the polymorphism in the population: ICs cause the collapse of the population, but only BCs can restore it. Vice-versa, catastrophes also appear to be a mechanism by which polymorphism is maintained, as they are crucial to prevent ICs from completely overtaking the population.

Interestingly, after mutations were stopped, populations were always observed to undergo only one catastrophe at most (Fig 7A), suggesting that *de novo* mutation might be needed to reintroduce ICs in the population after a catastrophe for continued population cycles. An additional role of mutation could be that it fuels the gradual replacement of weakly ICs by stronger imbalanced, more competitive ones, which increase the vulnerability of the population to collapse. Moreover, newly generated mutants could introduce additional randomness to the system, thus weakening the stabilizing force of negative frequency-dependence and increasing the probability of a catastrophe. Both hypotheses are supported by the observation that a

reduction of the mutation rate decreases the frequency of catastrophes (S10A and S10B Fig). The role of randomness is further emphasized by the fact that the frequency of catastrophes is reduced in the environment with consistent glucose availability (constant T_{off}, S10C Fig). Another possibility is that continuously generated mutants affect the glucose profile in the chemostat in such a way as to add a slight fitness advantage to ICs. According to this scenario, during the mutation-on segment of the simulation the fraction of ICs would tend to increase, periodically causing catastrophes, but the absence of mutants would make fitness of ICs and BCs more equal, and protected polymorphism would not allow the fraction of ICs to deviate too much from equilibrium to cause a catastrophe. This possibility is supported by the finding that the genotypes with the fitness advantage during the mutation-on segment are different from the ones during the mutation-off segment (S11 Fig).

Discussion

Upon transition to high glucose, 7 % of WT yeast cells enter a non-viable state of imbalanced glycolysis, whereby UG outpaces LG and glycolytic intermediates accumulate at low ATP [3]. Computational modeling studies suggested that the two states, balanced and imbalanced, are an inherent feature of glycolysis: the pathway can be pushed towards either one of the alternative states by spontaneous heterogeneity in metabolite concentrations or enzyme levels among isogenic cells [3]. Furthermore, it has also been shown that the propensity of the simulated yeast glycolysis pathway to enter the imbalanced state can be modified by slowing down UG, speeding up LG or phosphate transport from the vacuole. In this study we address the question why yeast cells do not employ available mechanisms, such as increasing the constitutive expression of LG or phosphate transport enzymes, to minimize or entirely eliminate the risk of developing metabolic imbalance. Although it is conceivable that the cost of these mechanisms to the population do not weigh up against the substantial benefit of rescuing 7 % of cells, we propose an alternative hypothesis, whereby WT yeast are prone to imbalanced glycolysis because they are evolutionarily optimized for scarce or varying glucose. Our simulations support this hypothesis: since the likelihood of entering the imbalanced state decreases with decreasing glucose concentration, model cells that evolve under scarce glucose exhibit higher expression of UG enzymes at the expense of LG enzymes to enhance glucose uptake and thus gain a competitive advantage without the risk of becoming imbalanced. However, the adaptation to scarce resource makes them more vulnerable to imbalanced dynamics when glucose is available abundantly.

Furthermore, in variable environments with rapidly fluctuating glucose levels, the seemingly maladaptive imbalanced state provided a clear fitness advantage over balanced metabolism: during the period of glucose abundance, ICs quickly accumulated FBP as intracellular storage that was then consumed during the period of scarcity to maintain high ATP and reproduce. Note that this benefit can only materialize if the imbalanced state is reversible. Experimental observations of yeast cells trapped in the imbalanced state show that they can accumulate substantial amounts of FBP (70 mM over 5 h in Hohmann et al. [9]), are viable for around 7 h and can resume growth on galactose when glucose is removed [3]. This suggests that metabolic balance is restored in these cells, and that FBP accumulated during the imbalanced period could be used by cells for growth after the removal of the imbalance. Our model indicates that imbalanced metabolism can be favored by selection because ICs can evolve higher levels of UG enzymes at the expense of LG enzymes to secure the resource faster than BCs without compromising the overall performance of the glycolysis pathway. (It should be noted that a cell in the imbalanced state will have a smaller flux through UG (v_{up}) than the same cell in the balanced state due to smaller ATP levels [24], a consequence of Eq 1. However,

Eq 1 also shows that lower levels of ATP can be compensated for, and v_{up} increased, by increasing $v_{max,up}$, i.e., by higher expression levels of UG enzymes that in our model are realized by cells of different genotypes. In other words, an IC with higher UG enzyme levels can have a higher flux through UG than a BC with a different genotype.) However, in environments with long periods of resource scarcity, ICs lost their fitness advantage over BCs. Since glucose uptake and cell growth are separated in time in ICs, and because the amount of glucose taken up by a cell depends on its volume, ICs do not increase their total capacity for processing glucose as they are securing it from the environment. BCs, on the other hand, show a clear accelerating growth pattern: because BCs grow at the same time as they take up glucose, increase in cell volume immediately translates into an increase in the total metabolic capacity of the cell. As a consequence, BCs grow more efficiently than ICs when the periods of glucose availability are long (i.e., environmental fluctuations are slow). One way to experimentally test the predictions of our model is to evolve yeast under different glucose availability regimes and determine the fraction of evolved cells that become imbalanced upon a transition to high glucose [3]. In addition, the expression levels of UG and LG enzymes in evolved strains could be quantified and compared against the patterns predicted by our model.

As mentioned above, stochastic phenotype determination, triggered by random fluctuations in metabolic state, provides a mechanism that explains the co-occurrence of balanced and imbalanced WT cells in an isogenic population upon the transition to excess glucose [3]. Our model suggests two other mechanisms that can also support a phenotypic polymorphism of BCs and ICs, which may be particularly important under natural conditions in a genetically variable population. First, our simulations show that both balanced and imbalanced dynamics represent viable strategies in an environment where the availability of glucose varies over time. Although, in any particular environment, one of the two strategies typically enjoys a competitive advantage over the other, the fitness differences between them are often small, such that substantial variation can be maintained under mutation-selection balance, whereby the rate at which less fit mutants are eliminated equals to the rate of their creation by mutation [22]. In our simulated populations, one type of cell is easily produced from another type by mutation, and since the evolvable parameters represent expression levels of enzymes, it is feasible that similar conversions could easily occur in natural populations.

The second mechanism that allows for phenotypic variation is negatively frequency-dependent selection, which can support the emergence and stable coexistence of discrete clusters of genetically differentiated BC and IC types. This protected polymorphism arises in a chemostat regime where cells compete for glucose, and their utilization strategy influences the resource concentration in the chemostat chamber. This establishes an ecological feedback: by consuming glucose in different ways, BCs and ICs induce a different dynamic of the glucose concentration, which, in turn, affects the two competing strategies in different ways. In fact, BCs create conditions favorable for the growth of ICs, and *vice versa*, such that each type enjoys an advantage of rarity, and thus diversity is maintained. Negative frequency-dependent selection has been previously experimentally demonstrated in yeast populations in multi-resource environments [25, 26], and in models of a single resource environment with a branching metabolic pathway (fermentation vs. respiration) [27]. Our simulations, however, point to the possibility of protected polymorphism in a single resource chemostat environment with a linear metabolic pathway. One way to experimentally demonstrate protected polymorphism could be to establish under what conditions already evolved BCs and ICs can stably coexist in a chemostat. Such experiments are lacking because laboratory studies generally work with well-characterized genetically monomorphic populations.

A further unanticipated phenomenon highlighted by our model is that a population of coexisting BCs and ICs under varying glucose can exhibit catastrophic collapses, often

followed by a recovery. A prelude to a catastrophe is an increase in the fraction of strongly ICs in the population due to their competitiveness. However, ICs in such a population become vulnerable to falling into a self-sustaining state of accumulating more FBP than they can use to produce ATP, which reduces their efficiency of growth, causes a drop in the population size with a concomitant increase in glucose concentration in the environment that pushes even more ICs into persistent imbalance. The recovery of the population depends on the presence of BCs, either surviving ones or newly generated mutants, that benefit from the increased glucose concentration in the environment. By restoring the normal glucose level, however, BCs create ecological conditions in which ICs are competitively superior, setting the stage for the cycle to repeat itself. Therefore, the recurrent catastrophic collapse and recovery of the population requires a polymorphism of balanced and imbalanced cells, but also helps to maintain their dynamic coexistence. Although in our simulations the recurrent catastrophes require mutational pressure, it is feasible that, under different conditions, they could occur without it and be the only mechanism to maintain polymorphism. Such a process would be akin to protected polymorphism with the difference that the decrease of fitness of dominant ICs would be delayed and dependent on chance, i.e. would only happen when a catastrophe is triggered by stochastic increase of glucose concentration due fluctuations in the population size.

The catastrophic eco-evolutionary dynamics observed in our simulations bears similarity to the phenomena of the tragedy of the commons and evolutionary suicide, particularly in cases when the population does not recover after a collapse. The tragedy of the commons occurs when individual-level adaptations driven by natural selection maximizes fitness relative to other individuals at the expense of a public good, which can result in decrease of mean population fitness (or a proxy thereof, such as overall offspring production) [28]. The resulting decrease in size can make the population vulnerable to extinction due to demographic or environmental stochasticity, or, alternatively, if the disturbance pushes the population into a different stable state associated with a different regime of selection (e.g. past a bifurcation point), the population may undergo evolutionary suicide, i.e. can be driven towards extinction deterministically by natural selection [29, 30]. In the context of the current model, high resilience of the population to fluctuations in glucose concentration, and thus to catastrophes, can be considered as public good for ICs. Yet, their individual-level adaptations, driven by the selective pressure to increase competitiveness by becoming more imbalanced, undermines this common good, pushing the population ever closer towards the brink of collapse.

We have focused our analysis on glycolytic imbalance in yeast, while drastically simplifying known aspects of its metabolism and regulatory architecture. Therefore, our analysis must not be interpreted to provide quantitatively accurate predictions, but rather to inspire novel insight and hypotheses for interpreting metabolic imbalance from an eco-evolutionary perspective. Our results may extend to other species that differ from yeast in their detailed metabolic make-up, but that face similar challenges in optimizing their growth to conditions of limited or ephemeral resource availability. Overall, our study demonstrates that a highly simplified metabolic pathway, without even considering its genetic regulation, is sufficiently flexible to encapsulate a dynamic feedback between metabolic adaptation and resource availability and that their interplay, in turn, gives rise to population level phenomena, such as the maintenance of alternative strategies or population cycles that shape selection on the metabolic pathway. Here, we have shown how considering this eco-evolutionary perspective sheds new light on the prevalence of substrate-accelerated death in yeast. We expect that it will do similarly well in explaining other seemingly maladaptive aspects of cellular metabolism.

Supporting information

S1 Text. A list of symbols and analysis of fitness of balanced and imbalanced cells in variable environments.
(PDF)

S1 Fig. Average volume increase rate of a BC during an environmental cycle, W_b (blue), becomes larger than that of an IC, W_i (orange) as the cycle length T increases (see S1 Text). The plots are shown for representative parameter values observed in NCG simulations: $v^{+}_{atp,g} = 6.3\ \text{mM} \cdot\ \text{min}^{-1}$, $q = 0.77$, $a = 3.8\ \text{mM} \cdot \text{min}^{-1}$, $V_0 = V_c$.
(TIFF)

S2 Fig. Optimization of the core glycolysis pathway in the absence of competition for glucose under NCG conditions with a constant glucose supply concentration, when the costs of UG and LG differ markedly. (A) UG is less costly, $w_{up} = 0.1$, $w_{lo} = 1$, (B) LG is less costly, $w_{up} = 1$, $w_{lo} = 0.1$. Each dot represents the average of an evolving genotype parameter ($v_{max,up}$, $v_{max,lo}$, k_{atp} and k_p) or a measure of balancedness at the end of an evolutionary simulation (t_e). Genotype parameter averages were computed over the entire population of cells; balancedness values $B_{g,1}$, $B_{g,2}$ were averaged over a randomly selected subpopulation of cells that were tracked individually. Results of 5 replicate simulations are shown for each of the studied [Glc] value.
(TIFF)

S3 Fig. Optimization of the core glycolysis pathway in the absence of competition for glucose under NCG conditions with an alternating glucose availability consisting of ON ($[Glc]_0$ = 2 mM) and OFF ($[Glc]_0 = 0.01$ mM) phases of equal duration with period $T = T_{on} + T_{off}$, when (A) no depletion of phosphate from the vacuole occurs, $K_{vac} \to \infty$, (B) the cost of phosphate transport is small, $w_p = 0.1$, (C) cell health does not decrease, $t_d \to \infty$, and therefore cells do not die, and (D) the alternative cost function is used (Eq 13). Each dot represents the average of an evolving genotype parameter ($v_{max,up}$, $v_{max,lo}$, k_{atp} and k_p) or a measure of balancedness at the end of an evolutionary simulation (t_e). Genotype parameter averages were computed over the entire population of cells; balancedness values $B_{g,1}$, $B_{g,2}$ were averaged over a randomly selected subpopulation of cells that were tracked individually, and $B_{p,phs}$ was calculated for the subset of tracked cells that survived through at least one ON and one OFF phase. Results of 5 replicate simulations are shown for each of the studied [Glc] and T value.
(TIFF)

S4 Fig. Optimization of the core glycolysis pathway in the absence of competition for glucose under NCG conditions with an alternating glucose availability consisting of ON ($[Glc]_0$ = 2mM) and OFF ($[Glc]_0$ = 0.01mM) phases of equal duration with period $T = T_{on} + T_{off}$ (see Fig 2B). Each dot represents the average of a flux v_{up}, v_{atp}, $v_{atp,e}$ over an environmental cycle, or the time when [FBP] falls below 5 mM (i.e., is used up) after the beginning of the OFF phase, t_{fbp}. The averages were computed over a randomly selected subpopulation of cells that were tracked individually at the end of an evolutionary simulation (t_e) and that survived through at least one ON and one OFF phase. Results of 5 replicate simulations are shown for each of the studied T value. The black line indicates $t_{fbp} = T_{off} = \frac{1}{2}T$, i.e. where FBP is used up exactly at the end of the OFF phase.
(TIFF)

S5 Fig. Overview of the average phenotypic balancedness $\overline{B}_{p,cov}$ and its standard deviation $s(B_{p,cov})$ of evolved tracked cells (colorbar) at the end of an evolutionary simulation (t_e) with

constant T_{off} for a wide range of glucose cycle length T and chemostat flow rate D values. A group of three or less circles represents three replicate simulations for the same pair of T and D values (i.e., circles have been displaced in the vertical direction for the purpose of visualization; a D value of the group is at the closest tick mark on the vertical axis). A circle in the plot is absent when the population did not survive to the simulation end, or the population size $N(t_e) < 1000$. Black dots indicate simulations where catastrophic dynamics was observed (see Section *Evolution of increased imbalancedness*. . .). High variation in balancedness of cells at $T = 20$ min, $D = 2 \times 10^{-3}$ min^{-1} and $D = 3 \times 10^{-3}$ min^{-1} is caused by evolved cells whose metabolite dynamics oscillates with period $2T$, i.e. twice as large as that of glucose pulse. These cells switch phenotype between imbalanced dynamics during one glucose cycle, and balanced dynamics during the cycle afterwards (S9 Fig). Because $B_{p,cov}$ is defined over an equal number of ON and OFF phases (see *Model and methods*), balancedness of a cell with switching phenotype depends on how many balanced and imbalanced cycles the cell went through and therefore is highly variable. Other high $s(B_{p,cov})$ values are caused by a few similar genotypes surviving at the end of the simulation due to their similar fitness (akin to the situation in Fig 4, $T = 120$ min).
(TIFF)

S6 Fig. Overview of the average phenotypic balancedness $\overline{B}_{p,cov}$ and its standard deviation $s(B_{p,cov})$ of evolved tracked cells (colorbar) at the end of an evolutionary simulation (t_e) with constant T_{off} for intermediate values of glucose cycle length T and chemostat flow rate D values. In this range, dimorphism and catastrophic dynamics in the population have often been observed. A group of three or less circles represents three replicate simulations for the same pair of T and D values (i.e., circles have been displaced in the vertical direction for the purpose of visualization; a D value of the group is at the closest tick mark on the vertical axis). A circle in the plot is absent when the population did not survive to the simulation end, or the population size $N(t_e) < 1000$. Black dots indicate simulations where catastrophic dynamics has been observed (see Section *Evolution of increased imbalancedness*. . .). A black dot without a circle indicates that the population has been wiped out by a catastrophe. Points of high variation in balancedness indicate stable dimorphism in the population, i.e. where both ICs and BCs stably coexist, except for cells at $T = 90$ min, $D = 3.8 \times 10^{-3}$ min^{-1} (lower circle) that show phenotype switching (see S5 Fig), and cells at $T = 80$ min, $D = 3.4 \times 10^{-3}$ min^{-1}, where two types of BCs stably coexist.
(TIFF)

S7 Fig. Overview of the average phenotypic balancedness $\overline{B}_{p,cov}$ and its standard deviation $s(B_{p,cov})$ of evolved tracked cells (colorbar) at the end of an evolutionary simulation (t_e) with varying T_{off}, CV(T_{off}) = 5 %, for a wide range of glucose cycle length T and chemostat flow rate D values. A group of three or less circles represents three replicate simulations for the same pair of T and D values (i.e., circles have been displaced in the vertical direction for the purpose of visualization; a D value of the group is at the closest tick mark on the vertical axis). A circle in the plot is absent when the population did not survive to the simulation end, or the population size $N(t_e) < 1000$. Black dots indicate simulations where catastrophic dynamics has been observed (see Section *Evolution of increased imbalancedness*. . .). One point of high variation in balancedness of cells at $T = 100$ min, $D = 4 \times 10^{-3}$ min^{-1} (dark red) is a result of dimorphism in the population, i.e. where both ICs and BCs stably coexist (Fig 5). A black dot without a circle indicates that the population has been wiped out by a catastrophe. The red dot indicates a simulation where stable dimorphism after t_{me} has been observed, but ICs have been later wiped out by a catastrophe, leaving only BCs in the population.
(TIFF)

S8 Fig. Overview of the average phenotypic balancedness $\overline{B}_{p,cov}$ and its standard deviation $s(B_{p,cov})$ of evolved tracked cells (colorbar) at the end of an evolutionary simulation (t_e) with varying T_{off}, CV(T_{off}) = 5 %, for a narrow range of glucose cycle length T and chemostat flow rate D values. In this range, dimorphism and catastrophic dynamics in the population have often been observed. A group of three or less circles represents three replicate simulations for the same pair of T and D values (i.e., circles have been displaced in the vertical direction for the purpose of visualization; a D value of the group is at the closest tick mark on the vertical axis). A circle in the plot is absent when the population did not survive to the simulation end, or the population size $N(t_e) < 1000$. Black dots indicate simulations where catastrophic dynamics has been observed (see Section *Evolution of increased imbalancedness. . .*). A black dot without a circle indicates that the population has been wiped out by a catastrophe. Points of high variation in balancedness indicate stable dimorphism in the population, i.e. where both ICs and BCs stably coexist. Red dots indicate simulations where stable dimorphism after t_{me} has been observed, but ICs have been later wiped out by a catastrophe, leaving only BCs in the population. Interestingly, environments with varying T_{off} are more conducive to forming stable dimorphic populations, compared to the analogous environments with constant T_{off}, where often a monomorphic population of ICs evolves (S6 Fig). Thus it appears that variation in T_{off} is disadvantageous to ICs. This can be explained by the fact that at constant T_{off}, ICs evolve to optimize FBP accumulation so that it is used up just before the next cycle begins. Variation in T_{off} adds more risk to ICs that the accumulated FBP will not be fully used up during the OFF phase, thus decreasing their fitness and putting them at a disadvantage compared to BCs.
(TIFF)

S9 Fig. Metabolite and growth dynamics of cells with a switching phenotype, evolved in a chemostat at T = 20 min, constant T_{off} and $D = 3 \times 10^{-3}$ min^{-1}. Cell exhibits both imbalanced and balanced dynamics during different environmental cycles. This occurs because balancedness of glycolysis in the model depends on [P_i] in the cytosol upon activation with glucose at the beginning of the ON phase (see Introduction). (A) Regular phenotype switching. Imbalanced cycle starts with lower P_i, however, due to usage of accumulated FBP, P_i increases in the cytosol at the end of the cycle, which results in the next cycle being balanced. During the balanced cycle, there is no FBP accumulation in the cytosol, P_i drops at the end of the cycle, and the next cycle becomes imbalanced again. (B) Irregular phenotype switching.
(TIFF)

S10 Fig. Population dynamics in chemostat simulations has less catastrophic events (compared to the dynamics shown in Fig 7A, variable T_{off}, $\overline{T} = 100$ min, CV(T_{off}) = 5 %, $D = 4 \times 10^{-3}$ min^{-1} and $\mu = 1 \times 10^{-2}$) when the mutation rate is lower, (A) $\mu = 1 \times 10^{-3}$, (B) $\mu = 5 \times 10^{-4}$, or when (C) T_{off} is constant. Yellow background indicates the mutation-off segment of the simulation. In populations shown in (A) and (B), dimorphism as in Fig 5 evolves.
(TIFF)

S11 Fig. Distribution of genotypic balancedness $B_{g,1}$ of tracked cells in time in the simulation shown in Fig 7. During a catastrophe event, the distribution shifts toward more BCs. At the end of the simulation, the population is dimorphic (see Fig 5).
(TIFF)

S1 Video. Average reproduction rate r of tracked cells during an environmental cycle plotted against their phenotypic balancedness $B_{p,phs}$ during the whole length of a simulation in

the NCG scenario with alternating glucose supply, T = 40 min (see legend of Fig 4). Yellow background indicates the mutation-off segment of the simulation.
(WEBM)

S2 Video. Average reproduction rate r of tracked cells during an environmental cycle plotted against their phenotypic balancedness $B_{p,phs}$ during the whole length of a simulation in the NCG scenario with alternating glucose supply, T = 120 min (see legend of Fig 4). Yellow background indicates the mutation-off segment of the simulation.
(WEBM)

S3 Video. Average reproduction rate r of tracked cells during an environmental cycle plotted against their phenotypic balancedness $B_{p,phs}$ during the whole length of a simulation in the NCG scenario with alternating glucose supply, T = 200 min (see legend of Fig 4). Yellow background indicates the mutation-off segment of the simulation.
(WEBM)

S4 Video. Evolution of a dimorphic population. Each dot represents the average reproduction rate r of a tracked cell averaged during an environmental cycle plotted against its phenotypic balancedness $B_{p,cov}$ during a simulation in a chemostat with a variable OFF phase, $\overline{T} = 100$ min, $T_{on} = 1$ min, $\overline{T}_{off} = 99$ min, CV(T_{off}) = 5 %, and $D = 4 \times 10^{-3}$ min^{-1} (see legend of Fig 5). Yellow background indicates the mutation-off segment of the simulation. Catastrophic crashes and recoveries of the population are visible as abrupt jumps in reproduction rate and balancedness (see also Fig 7). At the end of the simulation, subpopulations of BCs and ICs coexist at a stable equilibrium frequency.
(WEBM)

S1 Model. A CellML model of a yeast cell with a core glycolysis pathway.
(CELLML)

Acknowledgments

Albertas Janulevicius and G. Sander van Doorn thank David Ekkers for inspiring discussions.

Author Contributions

Conceptualization: Albertas Janulevicius, G. Sander van Doorn.

Formal analysis: Albertas Janulevicius, G. Sander van Doorn.

Funding acquisition: G. Sander van Doorn.

Investigation: Albertas Janulevicius.

Software: Albertas Janulevicius.

Visualization: Albertas Janulevicius.

Writing – original draft: Albertas Janulevicius.

Writing – review & editing: Albertas Janulevicius, G. Sander van Doorn.

References

1. Appling DR, Anthony-Cahill SJ, Mathews CK. Biochemistry: Concepts and Connections. First global ed. Pearson; 2016.

2. Teusink B, Walsh MC, van Dam K, Westerhoff HV. The danger of metabolic pathways with turbo design. Trends in Biochemical Sciences. 1998; 23(5):162–169. https://doi.org/10.1016/S0968-0004(98)01205-5 PMID: 9612078

3. van Heerden JH, Wortel MT, Bruggeman FJ, Heijnen JJ, Bollen YJ, Planqué R, et al. Lost in transition: start-up of glycolysis yields subpopulations of nongrowing cells. Science. 2014; 343(6174):1245114. https://doi.org/10.1126/science.1245114 PMID: 24436182

4. Van Aelst L, Hohmann S, Bulaya B, de Koning W, Sierkstra L, Neves MJ, et al. Molecular cloning of a gene involved in glucose sensing in the yeast Saccharomyces cerevisiae. Molecular Microbiology. 1993; 8:927–943. https://doi.org/10.1111/j.1365-2958.1993.tb01638.x PMID: 8355617

5. Thevelein JM, Hohmann S. Trehalose synthase: guard to the gate of glycolysis in yeast? Trends in Biochemical Sciences. 1995; 20:3–10. https://doi.org/10.1016/S0968-0004(00)88938-0 PMID: 7878741

6. Postgate JR, Hunter JR. Acceleration of bacterial death by grown substrates. Nature. 1963; 198:273. https://doi.org/10.1038/198273a0 PMID: 13985692

7. Calcott PH, Montague W, Postgate JR. The levels of cyclic AMP during substrate-accelerated death. Journal of General Microbiology. 1972; 73:197–200. https://doi.org/10.1099/00221287-73-1-197 PMID: 4347342

8. Postma E, Verduyn C, Kuiper A, Scheffers WA, van Dijken JP. Substrate-accelerated death of *Saccharomyces cerevisiae* CBS 8066 under maltose stress. Yeast. 1990; 6:149–158. https://doi.org/10.1002/yea.320060209 PMID: 2183522

9. Hohmann S, Bell W, Neves MJ, Valckx D, Thevelein JM. Evidence for trehalose-6-phosphate-dependent and -independent mechanisms in the control of sugar influx into yeast glycolysis. Molecular Microbiology. 1996; 20:981–991. https://doi.org/10.1111/j.1365-2958.1996.tb02539.x PMID: 8809751

10. Betz A, Moore C. Fluctuating metabolite levels in yeast cells and extracts, and the control of phosphofructokinase activity in vitro. Archives of Biochemistry and Biophysics. 1967; 120:268–273. https://doi.org/10.1016/0003-9861(67)90238-X PMID: 4226719

11. Teusink B, Passarge J, Reijenga CA, Esgalhado E, van der Weijden CC, Schepper M, et al. Can yeast glycolysis be understood in terms of in vitro kinetics of the constituent enzymes? Testing biochemistry. European Journal of Biochemistry. 2000; 267:5313–5329. https://doi.org/10.1046/j.1432-1327.2000.01527.x PMID: 10951190

12. Thomas MR, O'Shea EK. An intracellular phosphate buffer filters transient fluctuations in extracellular phosphate levels. Proceedings of the National Academy of Sciences of the United States of America. 2005; 102:9565–9570. https://doi.org/10.1073/pnas.0501122102 PMID: 15972809

13. van Heerden JH, Bruggeman FJ, Teusink B. Multi-tasking of biosynthetic and energetic functions of glycolysis explained by supply and demand logic. BioEssays. 2015; 37:34–45. https://doi.org/10.1002/bies.201400108 PMID: 25350875

14. Bryan AK, Goranov A, Amon A, Manalis SR. Measurement of mass, density, and volume during the cell cycle of yeast. Proceedings of the National Academy of Sciences of the United States of America. 2010; 107:999–1004. https://doi.org/10.1073/pnas.0901851107 PMID: 20080562

15. Dekel E, Alon U. Optimality and evolutionary tuning of the expression level of a protein. Nature. 2005; 436(7050):588–592. https://doi.org/10.1038/nature03842 PMID: 16049495

16. Boscá L, Corredor C. Is phosphofructokinase the rate-limiting step of glycolysis? Trends in Biochemical Sciences. 1984; 9(9):372–373.

17. Edelstein-Keshet L. Mathematical models in biology. SIAM: Society for Industrial and Applied Mathematics; 2005.

18. Verstrepen KJ, Klis FM. Flocculation, adhesion and biofilm formation in yeasts. Molecular Microbiology. 2006; 60:5–15. https://doi.org/10.1111/j.1365-2958.2006.05072.x PMID: 16556216

19. Press WH, Teukolsky SA, Vetterling WT, Flannery BP. Numerical recipes. The art of scientific computing. 3rd ed. Cambridge University Press; 2007.

20. Uchida M, Sun Y, McDermott G, Knoechel C, Le Gros MA, Parkinson D, et al. Quantitative analysis of yeast internal architecture using soft X-ray tomography. Yeast. 2011; 28:227–236. https://doi.org/10.1002/yea.1834 PMID: 21360734

21. Tyson CB, Lord PG, Wheals AE. Dependency of size of *Saccharomyces cerevisiae* cells on growth rate. Journal of Bacteriology. 1979; 138:92–98. https://doi.org/10.1128/JB.138.1.92-98.1979 PMID: 374379

22. Smith J. Evolutionary genetics. Oxford University Press; 1998.

23. Metz JAJ, Mylius SD, Diekmann O. When Does Evolution Optimize? Evolutionary Ecology Research. 2008; 10:629–654.

24. Luyten K, de Koning W, Tesseur I, Ruiz MC, Ramos J, Cobbaert P, et al. Disruption of the Kluyveromyces lactis GGS1 gene causes inability to grow on glucose and fructose and is suppressed by mutations that reduce sugar uptake. European Journal of Biochemistry. 1993; 217:701–713. https://doi.org/10.1111/j.1432-1033.1993.tb18296.x PMID: 8223613

25. Charlebois DA, Balázsi G. Frequency-dependent selection: a diversifying force in microbial populations. Molecular Systems Biology. 2016; 12:880. https://doi.org/10.15252/msb.20167133 PMID: 27487818

26. Healey D, Axelrod K, Gore J. Negative frequency-dependent interactions can underlie phenotypic heterogeneity in a clonal microbial population. Molecular Systems Biology. 2016; 12:877. https://doi.org/10.15252/msb.20167033 PMID: 27487817

27. Wortel MT, Bosdriesz E, Teusink B, Bruggeman FJ. Evolutionary pressures on microbial metabolic strategies in the chemostat. Scientific Reports. 2016; 6:29503. https://doi.org/10.1038/srep29503 PMID: 27381431

28. Rankin DJ, Bargum K, Kokko H. The tragedy of the commons in evolutionary biology. Trends in Ecology and Evolution. 2007; 22:643–651. https://doi.org/10.1016/j.tree.2007.07.009 PMID: 17981363

29. Rankin DJ, López-Sepulcre A. Can adaptation lead to extinction? Oikos. 2005; 111(3):616–619. https://doi.org/10.1111/j.1600-0706.2005.14541.x

30. Webb C. A complete classification of Darwinian extinction in ecological interactions. The American Naturalist. 2003; 161:181–205. https://doi.org/10.1086/345858 PMID: 12675367